Abstract

Purpose: Fine sediment has been shown to be a major cause of the degradation of lakes and rivers, and as a result research has been directed towards the understanding of fine sediment dynamics and the minimisation of sediment inputs. The use of tracers within a sediment fingerprinting framework has become a heavily used technique to investigate the sources of fine sediment pressures. When combined with the use of historically deposited sediment the technique provides the opportunity to reconstruct past changes to the environment. However, alterations to tracer signatures during sediment transport and storage are a major potential source of uncertainty associated with tracer use. At present few studies have quantified the uncertainties associated with tracer use.

Materials and methods: This paper investigated uncertainty by determining the differences between sediment provenance predictions obtained using lithogenic radionuclide, geochemical, and mineral magnetic signatures when fingerprinting lake and floodplain sedimentary deposits. It also investigated the potential causes of the observed differences.

Results and discussion: A reservoir core was fingerprinted with the least uncertainty, with tracer group predictions ~28% apart and a consistent down-core trend in changing sediment provenance produced. When fingerprinting an on-line lake core and four floodplain cores, differences between tracer group predictions were as large as 100%; the down-core trends in changing sediment provenance were also different. The differences between tracer group predictions could be attributed to the organic matter content and particle size of the sediment. There was also evidence of the in-growth of bacterially derived magnetite and chemical dissolution affecting the preservation of tracer signatures. Simple data corrections for sediment organic matter content and particle size did not result in significantly greater agreement between the predictions of the different tracer groups. Likewise the inclusions of weightings for tracer discriminatory efficiency and within source variability had minimal effects on the fingerprinting results.

Conclusions: This paper highlights the importance of tracer selection and the consideration of recognising tracer non-conservatism when using lake and floodplain sediment deposits to reconstruct anthropogenic changes to the environment and changing sediment dynamics. It was recommended that future research focus on the assessment of uncertainty using the

artificial mixing of sediment source samples, the limitation of the fingerprinting to narrow particle size fractions and the development of specific particle size and organic matter correction factors for each tracer.

1. Introduction

The use of tracers and sediment fingerprinting to determine sediment provenance have gained increasingly widespread adoption, with published papers on the subject growing at an almost exponential rate in recent years (Walling 2013). The principle of sediment fingerprinting is based upon a comparison of the properties of fine sediment transported or deposited by a river with the properties of the potential sediment sources present in a catchment (Klages and Hseih 1975). It relies on the ability of sediment sources to be differentiated on the basis of their properties, and the assumption that the properties of the sediment still reflect those of its sources, after it has been delivered to a river, floodplain or lake (Collins et al. 1997a). A wide variety of different tracers have been employed in the published literature, which include mineral magnetism, (Caitcheon 1993), lithogenic radionuclides (Gruszowski et al. 2003), geochemistry (Collins et al. 1997a) and particle size, shape and colour (Krein et al. 2003). The use of tracers within a sediment fingerprinting framework has been applied in a range of long term depositional environments, such as lakes and reservoirs (Foster et al. 1998), floodplains (Collins et al. 1997b) and floodplain lakes (Winter et al. 2001). Sediment fingerprinting has been used to identify the impacts of anthroprogenic changes to the environment, such as the erosion of man-made road verges (Collins et al. 2010) or changes in catchment land cover (Miller et al. 2005). Tracers also have a history of use as qualitative indicators of historical changes in sediment provenance (e.g. Oldfield *et al*. 1983; Foster *et al*. 2012).

Despite the widespread use of tracers and sediment fingerprinting, many uncertainties exist regarding the accuracy and reliability of results derived from using them. Foster and Lees (2000) identified key assumptions associated with fingerprinting contemporary sediment sources. These included an ability for the tracer to distinguish between at least two potential sediment sources of interest; that the tracer is transported and deposited in the same way as

the medium of interest (i.e. the sediment); that selective erosion does not change tracer properties (or that, if it does so, only in a way that is predictable) and that unmixing models can cope with the inherent variability in sediment source properties. These four assumptions underpin all tracer studies but Foster and Lees (2000) identified two further assumptions when using historically deposited sediments. These were the assumptions that post-depositional digenesis was minimal and that differences between source properties have not changed over the timescale of deposition.

The potential for tracer non-conservatism and uncertainties associated with tracer use have been widely discussed in the published literature. Changes to the particle size distribution of sediment (Thompson and Morton 1979) and the organic enrichment of sediment (Motha et al. 2003) are the most commonly cited reasons for tracer non-conservatism. The enrichment (Wang et al. 2010) and depletion (Nadeu et al. 2011) of sediment with organic matter has been shown to occur during erosion and sediment transport. Some tracers, e.g. heavy metals, have also been shown to be associated with the organic fraction (Hirner et al. 1990; Wallbrink et al. 1997) while others, such as magnetic susceptibility and remanence signatures, are diluted by it (Walden et al. 1999). Likewise relationships between tracer concentrations and the SSA of the sediment have often been shown in published literature (Horowitz and Elrick 1987; Foster et al. 1998; Bihari and Dezső 2008), resulting in changes to tracer concentrations as particle size is altered. When fingerprinting historically deposited sediment additional potential sources of tracer non-conservatism have been suggested to exist. These specifically include the in-growth of bacterially derived magnetic minerals (Oldfield 2007; Foster et al. 2008) or the dissolution of tracers by oxido-reduction reactions (Anderson and Rippey 1988).

At present a limited number of studies have explored tracer behaviour on the uncertainty associated with sediment provenance predictions when fingerprinting sedimentary deposits. The primary reason for this is that an independent source of sediment provenance information is usually not available for the validation of results, due to the absence of monitoring at the time of sediment deposition. This study attempts to overcome this limitation by fingerprinting

sediment cores using different tracer groups separately, and in various combinations, so that the differences between their provenance predictions can be quantified. The differences between predictions can then be compared to potential sources of tracer non-conservatism, such as organic enrichment, particle size effects or chemical alterations to determine the potential causes of the differences observed. On this basis the following objectives were produced:

1: To determine the differences between sediment provenance predictions obtained using lithogenic radionuclide, geochemical, and mineral magnetic signatures when fingerprinting lake and floodplain sedimentary deposits.

2: To investigate the impact of the organic enrichment of sediment, changes to its particle size distribution and post-depositional chemical and magnetic mineral alterations, on the observed differences between tracer group predictions.

2. Study catchment

The study was undertaken in the Nene basin; a lowland agricultural catchment of 1,634 km^2, located in the East Midlands, UK (Figure 1A). The maximum elevation is 226 m above Ordnance Datum (AOD) decreasing to 40 m AOD at Stanwick. The average annual rainfall recorded at Athorp and calculated over 140 years is 638 mm, with a standard deviation of 67mm. The catchment is underlain by Jurassic marine sedimentary deposits mostly comprising silts and clays with some outcrops of ironstone and limestone. Quaternary sand and gravel is found adjacent to the main river channel throughout the entire length of the basin, and glacial diamicton is found extensively at high altitude (Figure 1B). The 2007 UK Land Cover Map (Morton et al. 2011) indicates that the catchment land utilisation is 56% cultivated 22% pasture and 9% urban, the remaining 13% is composed of woodland, water and rough grassland. A comparison with the land cover of the catchment in the 1930s indicates that land cover at that time was approximately 50% pasture, 25% cultivated land, 3% urban, and the remaining 22% was composed of woodland, water and rough grassland

(Stamp, 1932). Flood defences protect the towns and villages along the main channel of the Nene and locks downstream of Northampton produce a navigable stretch of the river.

3. Material and methods

3.1. Sediment source sampling and sediment coring

Sediment sources were classified as channel banks, surface agricultural land and urban street dusts as these have been shown to be important sediment sources in UK catchments (Carter et al. 2003; Walling et al. 2007). The source sampling was distributed across the entire study area to account for variations in tracer concentrations associated with local geology (Figure 1B). A detailed breakdown of the distribution of source sampling is provided in the online supplementary material (Supplementary table 1). A total of 333 source samples were collected, 247 of which were from surface agricultural sources, 65 were from channel banks and 21 were from urban street dusts. Grassland was not used as a sediment source group as there was very little grassland present in the catchment which did not show evidence of having been cultivated in the past. As a result there was almost no ability of the tracers used to discriminate between cultivated and grassland.

Samples of topsoil were collected from the top 2 cm of the profile using a non-metallic trowel. Urban street dusts were collected from the material deposited at the side of both major and minor roads following the methods of Charlesworth and Foster (2005). Channel bank samples were collected from the lower and middle horizons of visibly eroding channel banks using a non-metallic trowel. The outermost exposed 2 cm of material were removed prior to sampling in order to minimise contamination from displaced surface material or deposited fluvial sediments. All samples were composed of an amalgamation of five sub samples taken from within a 15 m radius of each sampling point, to further increase the sample size.

A total of two lake cores and four floodplain cores were collected from the sites shown in Figure 1. Cores were retrieved from Sywell reservoir and an on-line (*sensu* Foster 2006) floodplain lake at Stanwick, using a 'mini-Mackereth' pneumatic corer (Mackereth 1969). Cores were collected in transparent Perspex tubes of ~5 cm internal diameter and 1 m length using the methods described by Foster and Walling (1994) and were maintained in a vertical position during transport to the laboratory.

A core was retrieved from each of the floodplain sampling sites shown in Fig. 1 using a steel percussion corer of ~6 cm internal diameter and 75 cm length. The core tube was manually driven into the floodplain surface using a sledge hammer and was retrieved using a tripod and chain hoist. On retrieval, the cores were retained in the corer during transport to the laboratory.

Down-core plots of ^{137}Cs activity were produced for each core (Figure 2). Peaks in activity in each core occur at a depth of 14 to 34 cm, these peaks are commonly attributed to the peak in fallout occurring at 1963 (Foster 2006). Provided that sediment accumulation rates did not significantly change due to changes in land use prior to 1963, the sediment contained within each core will have accumulated over the last ~ 50 – 150 years.

3.2.   Laboratory analyses

On return to the laboratory the lake cores were extruded vertically and sectioned using a slicing plate into 1 cm slices. Floodplain cores were sectioned into 2 cm slices. The sediment and source samples were oven dried at 40 °C and manually dis-aggregated with a pestle and mortar. The source samples were sieved to <63 µm to achieve a particle size distribution roughly comparable to that of the deposited sediment (Collins et al. 1997a).

The soil and sediment samples were analysed for a range of mineral magnetic, radionuclide and geochemical signatures providing three independent groups of tracer properties. Additionally, organic matter content and particle size analysis were undertaken on all sources and deposits.

Mineral magnetic signatures were measured using approximately 10 g of the source and sediment samples packed to a depth of ~2 cm in 10 ml sample pots. The following mineral magnetic signatures were measured: Low frequency susceptibility (χlf), frequency dependent susceptibility (χfd), susceptibility of ARM (χarm), soft Isothermal remanent magnetisation (IRM-100), saturation isothermal remanent magnetisation, (SIRM), and hard isothermal remanent magnetisation (HIRM) using a Bartington Instruments (Witney, UK) MS2b sensor, Molspin® anhysteretic remanent magnetiser, Molspin® pulse magnetiser, and a Molspin® (Witney, UK) slow-speed spinner magnetometer following the methods of Foster et al. (2008).

To measure radionuclide activity 3 g of source and sediment sample was packed to a depth of 4 cm in PTFE sample pots and sealed with a turnover cap and paraffin wax. All samples were left to equilibrate for a period of 21 days to allow for ingrowth of ^{222}Ra. Sediment samples were measured for a minimum of two days (>172,800s) and source samples for a minimum of one day (>86,400s) using Ortec EG&G (Tennessee, USA) hyper-pure Ge gamma detectors in a well configuration. Activities of ^{226}Ra, ^{234}Th, ^{235}U, ^{214}Pb, ^{228}Ac, ^{212}Pb, ^{40}K and ^{137}Cs were then determined using the methods of Wallbrink *et al.* (2003) and Foster *et al.* (2007).

Geochemical element concentrations were determined using 0.8 g $^+/_-$ 0.05g of each sample which was microwave digested at 180°C using *aqua regia.* Concentrations of Al, As, Ba, Ca, Co, Cr, Cu, Fe, Ga, Gd, K, La, Mg, Mn, Na, Nd, Ni, P, Pb, Ti, V, Y, Yb, Zn and Zr were determined using a Thermo Scientific (Waltham, USA) iCAP 6500 Duo View ICP-OES.

Sample particle size was determined using *ca.* 0.1 g sub-samples of sediment which were pre-treated with 10 ml of 30% hydrogen peroxide to remove organic matter. Each sample was placed into 5 ml of hydrogen peroxide for 24 hours at room temperature before being heated at 70 °C for four hours. The samples were then dispersed with 5 ml of 3% sodium hexametaphosphate solution combined with two minutes of ultrasonic treatment (Gray et al. 2010). A Malvern Instruments (Worcestershire, UK) laser granulometer with Hydro-2000 sample injection unit was used to determine the specific surface area (SSA) of each sample.

The organic content of 1-2 g sub-samples of sediment were determined using low temperature loss on ignition (LOI) in a Carbolite muffle furnace set at 450 °C for 4 hours. LOI was calculated using the pre combustion dry sample mass and the post combustion mass.

3.2.1. *Statistical determination of composite fingerprints*

The lithogenic radionuclides, geochemistry, and mineral magnetic tracer groups were used to fingerprint the sediment cores alone, in combinations of two groups, and as a final single group consisting of all tracers. The combinations of groups used are shown in Table 1, along with the abbreviation for each group used in future figures and tables.

A mass conservation test based upon that used by Collins et al. (1997) was firstly used to identify any tracers falling outside of the median +/- one median absolute deviation of the source groups shown in Table 2, the tracers failing this test are shown in Table 3. In addition it was found that a large number of tracers failed the mass conservation test in the Stanwick lake core above 19 cm depth, and the Upton floodplain core below 28 cm depth. For this reason the fingerprinting was only conducted on the sections above and below these depths.

A two-step statistical procedure based upon that used by Collins et al. (2012) was then used to select the optimum composite fingerprint for each tracer group at each coring location. Firstly a Kruskal–Wallis H test was used to remove any tracers which did not show a significant difference in concentration between at least two of the sediment sources (Table 4).

The selection of the optimum composite fingerprint was performed using the tracers passing the mass conservation test and Kruskal–Wallis H test. A Genetic Algorithm based Linear Discriminant Analysis (GA-LDA) was used to identify the optimum composite fingerprint for each tracer group in each core. Any composite fingerprint which failed to correctly discriminate between 80% of source samples was removed from further analysis, with the aim of minimising the uncertainty introduced by source discrimination, rather than tracer behaviour. A value of 80% was selected, as a review of published historically deposited

sediment fingerprinting studies (Collins *et al* 1997b; Owens *et al*. 1999; Miller *et al*. 2005; Collins *et al*. 2010) found that composite fingerprints were rarely used which failed to achieve at least this amount of discrimination. The composite fingerprints which were formed for each tracer group for each core are provided in Table 5.

3.2.2. *Unmixing modelling*

An unmixing model based upon that of Collins et al. (2010a) was used to apportion contributions from the sediment source groups (Equation 1). The model operates by minimising the sum of squares of the relative errors in the objective function (f) by changing the relative source proportions (P_s). Constraints were included in the model so that proportional source contributions were between 0 and 1 and the proportional source contributions summed to 1.

$$\text{(1)}$$

$$\sum_{i=1}^{n} \left\{ \left(C_i - \left(\sum_{s=1}^{m} P_s S_{si} Z_s O_s SV_{si} \right) \right) / C_i \right\}^2 W_i$$

Where, C_i = concentration of fingerprint property (i) in time-integrated suspended sediment sample

P_s = the optimised percentage contribution from source category (s)

S_{si} = median concentration of fingerprint property (i) in source category (s)

Z = particle size correction factor for source category (s)

O_s = organic matter content correction factor for source category (s)

SV_{si} = weighting representing the within-source variation of fingerprint property (i) in source category (s)

W_i = tracer discriminatory weighting;

n = number of fingerprint properties comprising the optimum composite fingerprint

m = number of sediment source categories.

Model uncertainty was determined using 3000 random tracer concentrations from within the median +/- one median absolute deviation of each source group, in a Monte Carlo uncertainty analysis.

The tracer discriminatory and within source variability weightings were applied to the model based on the methods used by Collins et al. (2010b) (Equations 2 and 3).

$$(2)$$

$$SV_{SI} = 1 - (\frac{\Sigma n \left(\frac{MAD}{Median}\right)}{n})$$

Where, SV_{si} = Within source tracer variability weighting

MAD = Median absolute deviation.

$$(3)$$

$$Wi = \frac{E_t}{E_a}$$

Where, W_i = tracer discriminatory weighting

E_t = Discriminatory efficiency of tracer

E_a = minimum discriminatory efficiency of any used tracer.

Laceby and Olley (2014) showed that the Sv_{Si} correction could heavily impact model performance. To account for this potential uncertainty, cores found to have large differences between tracer group predictions were fingerprinted a second time without the use of either the SV_{si} or W_i correction to determine the impacts of the weightings.

The average difference between tracer group fingerprint predictions in each core slice was quantified by subtracting the predicted contribution of one tracer group from the predicted contribution of the second tracer group, between the 5th and 95thpercentiles of the 3000 ranked

Monte Carlo results. The average difference between these 2700 Monte Carlo results for each slice of core was then taken as a quantitative expression of the differences between tracer group predictions. These differences were correlated in a Pearson Correlation analysis with LOI, SSA, and selected magnetic ratios which indicate the likely alteration of mineral magnetic signatures in the sediment. These ratios are described with the results.

3.2.3. *Particle size and Organic content corrections*

The fingerprinting was initially conducted without corrections for sediment organic matter content and particle size, so that the impacts of these potential causes of tracer non-conservatism could be identified. When the results suggested that organic matter and particle size were potentially responsible for differences between tracer group predictions, the unmixing modelling was repeated and incorporated these corrections. The corrections were applied from the beginning for the fingerprinting procedure, with the mass conservation test and determination of the optimum composite fingerprint repeated with the corrected tracer signatures. The corrected results were compared to the uncorrected results and the results produced by other tracer groups.

As it was found that the sediment cores were affected by down-core trends in organic matter and particle size distribution (Fig. 2), single number correction factors were considered unsuitable to represent the entire core. For this reason all sediment and source samples were given an individual correction factors, calculated using Equations 4 and 5, which were based upon the methods of Collins *et al*. (1997).

$$(4)$$

$$O_s = T\left(\frac{1}{1 - \left(\frac{LOI}{100}\right)}\right)$$

Where, O_s = organic matter content correction factor for source category (*s*)

T= measured tracer concentration

LOI= loss on ignition (%).

(5)

$$Z = \frac{T}{SSA}$$

Where, Z = particle size correction factor for source category (*s*)

T= measured concentration value

SSA= specific surface area.

4. Results and discussion

4.1. Sediment, organic matter content and particle size distribution

Prior to fingerprinting the sediment, down-core plots of LOI and SSA were constructed to provide an indication of changes to the organic matter content and particle size distribution of sediment during transport and post-depositional storage. LOI (Figure 3A) is enriched above the median LOI of surface agricultural and channel bank source samples in all cores other than Sywell reservoir and most of the Kingsthorpe floodplain core (Table 2). All cores show an up-core increase in LOI, with the core at Earls Barton showing a particularly large increase, and being composed predominantly of organic matter in the uppermost 6 cm of the core.

SSA (Figure 3B) is higher than the maximum sediment source group median of 1.18 m^2 g^{-1} in all cores except for the Kingsthorpe floodplain core, indicating a fining of sediment particle size. Most cores have a ~50% increase in SSA over the source group medians, although between a depth of 20 and 54 cm the Earls Barton core has over double the SSA of the source groups. It is therefore clear that LOI and SSA is significantly different from the source material in most of the cores.

In the semi-arid Karoo in South Africa Foster *et al.* (2005) found that a sediment core taken from a farm dam had a mean SSA of 0.89 m^2 g^{-1} and LOI of 3.22%. In comparison to the lake cores sampled from the Nene basin both the SSA and LOI are far lower. In lake Qarun in Egypt the LOI of the core is a mean of 9.09% and the SSA is a mean of 2.21 m^2 g^{-1} (Foster *et al* 2008) which are values comparable to many of the cores analysed in this study. In a lake core taken from Aqualate Mere, Central England the LOI exceeded 60%, reaching a value close to the Earls Barton floodplain core, whereas the SSA was between 0.8 and 1 being more comparable to the Kingsthorpe core (Pittam *et al.* 2008). It can therefore be established that the SSA and LOI values found in the Nene are not a-typical of cores sampled in other catchments worldwide however, in many other catchments SSA and LOI are often likely to be more representative of source samples sieved to <63µm.

4.2. Quantifying differences between the sediment provenance predictions of different tracer groups

To simplify the analysis only the predicted contributions from channel banks were compared, as this was suggested to be the dominant sediment source and its prediction was considered to be representative of the overall modelling results. The predicted contributions of sediment originating from urban street dusts made by the different tracer groups are provided in the online supplementary material (Supplementary figure 1). Predicted contributions from street dusts were negligible for most tracer groups in most cores, especially prior to the 1963 ^{137}Cs

peaks. Differences between the tracer group predictions were smallest in the Sywell reservoir core. The median predicted contributions from channel banks at the base of the core ranged from 31% made by 'All' tracer group up to 100% made by mineral magnetic signatures alone (Fig. 4A). In the middle and upper sections of the core, this difference decreased to between a 45% and 95% predicted contribution made by the different tracer groups. Most tracer groups show little change in predicted sediment provenance through the down-core profile, indicating a consistent trend in their predictions, although individual peaks and troughs do not consistently occur in the predictions made by all of the tracer groups.

In the other cores the differences between the predictions of the different tracer groups were larger than at Sywell. The Stanwick lake core (Fig.4B) had a difference in predictions of up to 100% between tracer groups containing mineral magnetic signatures and those containing geochemical tracers. All of the tracer groups in the Kingsthorpe floodplain core (Fig 4.C) predict widely different contributions of sediment from channel banks, ranging from between a 0% to a 95% median contribution. In this core two additional tracer groups were used (Mag fallout and Geochem fallout), these contained the fallout radionuclide ^{137}Cs. ^{137}Cs was able to be used because there was no indication of additional ^{137}Cs fallout after the peak centered upon 1963 (Figure 2). The fingerprints which used fallout radionuclides predicted a contribution most similar to mineral magnetic signatures, although differences of up to 23% were observed between the predictions of these two groups. The two fingerprint predictions for the Earls Barton core (Fig.4 D) showed a very similar down-core trend, however the predictions were up to up to 38% different. In the Upton floodplain core (Fig. 4E) the 'All' tracer group and Mag litho group predict that almost all sediment originated from channel banks. However, the Geochem fingerprint predicted a contribution 89% differently. Between a 22% to a 38% difference between predictions were found in the bottom two thirds of the Stanwick floodplain core (Fig. 4F), this difference increased to a maximum of a 64 % at the top of the core. Most tracer groups in the floodplain and floodplain lake cores predicted

different down-core trends. A summary table of all differences is provided in the online supplementary material (Supplementary table 3).

It was observed that the different tracer groups predicted contributions from urban street dusts far more similarly than from channel banks. It is likely that this results from the large contrasts in tracer concentrations between the street dust and other source groups, as was also found by Pulley *et al.* (2015) in relation to actively transported and recently deposited sediment in the Nene catchment. As a result large changes to tracer signatures through non-conservatism would be required to mask the sediment provenance signal of the street dust source group.

4.3. The impacts of weightings

The inclusion of the discriminatory and within source variability weightings had little impact on the predictions of most tracer groups in most cores (Table 6). Exceptions were the Geochem litho and Geochem tracer groups in the Kingsthorpe floodplain core. The uncertainty of the Geochem litho group increased but the median prediction was bought closer to that of the mineral magnetic and fallout radionuclide tracers. The Geochem group was significantly changed by the omission of weightings; uncertainty was reduced and the predictions were much more comparable to that of most other tracer groups. In the Stanwick floodplain core the application of weightings to the 'All' tracer group prediction, resulted in a smaller uncertainty and large change in sediment provenance prediction. However, the prediction does not come closer to that of the Geochem litho group. A general observation could also be made that the application of weightings does not reduce uncertainty in most of the unmixing models run.

4.4. The effects of changes to the sediment organic content, particle size distribution and chemical alterations of sediment on the tracer group provenance predictions

As changing sediment provenance is represented by the tracer fingerprint predictions, comparing individual tracer groups' provenance predictions to factors which can potentially cause tracer non-conservatism such as LOI, would likely provide some indication of the LOI of the changing sources of the sediment. Instead of this, the differences between the predicted contributions of sediment from channel banks made by two tracer groups were compared to potential causes of tracer non conservatism, as they were considered to be more representative of the error caused by tracer behaviour.

4.4.1. The organic enrichment of sediment

The Pearson correlation analysis (Table 7) showed that the differences between most tracer group predictions in the Kingsthorpe, Upton, and Stanwick floodplain cores and in the Sywell reservoir core are significantly correlated with the LOI of the sediment. In the Upton floodplain core and Sywell reservoir core, as LOI increases the predicted contribution of sediment from channel banks made by groups containing mineral magnetic signatures increases in relation to groups containing geochemical tracers. In the Kingsthorpe core, as LOI increases, mineral magnetic signatures predict lower contributions from channel banks than geochemical tracers, showing the opposite trend to Upton and Sywell. Table 2 shows that mineral magnetic signatures are lowest in concentration in channel banks, so a dilution of magnetic signatures by organic matter would be expected to cause an increase in the predicted contribution of sediment from channel banks. On this basis, it is suggested that the increased predicted contribution of sediment from channel banks made by mineral magnetic containing tracer groups in Upton and Sywell, when sediment LOI increases, could be due to the dilution of mineral magnetic signatures by organic matter as magnetic signatures are not associated with the organic fraction of the sediment (Lees 1999). Therefore this result is what would be

expected from mineral magnetic theory. The fact that a similar result was not encountered in the other cores analysed suggests that other causes of tracer non-conservatism are of more importance and are likely masking the impacts of organic matter dilution. Organic matter data corrections were applied to the Mag litho group in the Sywell, Stanwick lake, Kingsthorpe and Upton cores (see online supplementary figure 2 and supplementary table 4). It was found that the correction had very little impact on the predictions made in any core, suggesting that the dilution of magnetic signatures by organic matter had little effect on the fingerprinting results.

In the Kingsthorpe floodplain core there is an increase in the predicted contribution of sediment made by geochemical and lithogenic radionuclide tracers, in relation to mineral magnetic signatures, when LOI increases. An explanation for this may be a result of the association of geochemical or radionuclide tracers with the organic fraction. For example, calcium is used in most composite fingerprints in this core and is found in high concentrations in the channel bank source group in relation to the surface agriculture source group. Therefore, an increase in the concentration of Ca, caused by the enrichment of organic matter (Figure 3), would result in an increased predicted contribution from channel banks when the LOI of the sediment increases. Although it cannot be shown which tracers are associated with organic matter in the Nene using the available data, it has been shown in published literature that organic matter can concentrate between 1-10% of dry weight of Co, Cu, Fe, Pb, Mn, Mo, Ni, Ag, V, and Zn (Swanson et al. 1966). Charlesworth *et al*. (2003) showed that between 7.7% and 90.6% of Cd, Cu, Ni, Zn and Pb present in urban street dusts in Coventry, (a town close to Northampton in the English Midlands, UK) were concentrated within the organic fraction of urban street dusts. There exists therefore a large potential for the enrichment of geochemical tracers in the cores caused by the increased organic matter content of the sediment.

When the Geochem group was organic corrected in the Sywell, Kingsthorpe and Upton cores its prediction did not become significantly closer to those predictions made by the other tracer groups. In the Stanwick floodplain core the down-core trends predicted by the Geochem litho and 'All' groups were reversed by the correction. While it is unclear which result best represents the sediment provenance the correction clearly has a large impact on the fingerprinting results from this core. The lack of a clear improvement caused by the correction suggests that relationships between geochemical tracers and organic matter are not linear, as the corrections assume. The previously discussed association of tracers with the organic fraction of sediments is an example of such a non-linear relationship.

4.4.2. *Changes to sediment particle size*

The SSA of the sediment is highly correlated with most differences between the tracer groups' sediment provenance predictions in the Earls Barton, Stanwick and Upton floodplain cores (Table 7). In the Earls Barton floodplain core, as the SSA of the sediment increases, the prediction of the 'All' tracer group (containing geochemical tracers and ^{40}K decreases in relation to the prediction of the Geochem tracer group (Table 7E). ^{40}K has low activities in urban street dusts compared to the other sediment sources (Table 2). It can therefore be identified that any reduction in sediment ^{40}K activity caused by a change in sediment SSA would result in a greater predicted contribution from urban street dusts and a reduced contribution from the other sediment sources. However, published literature has shown ^{40}K to be concentrated within small clay minerals (Tsabaris et al. 2007), suggesting an inconsistency between the results found in the Nene and prior knowledge of tracer behaviour. An alternative explanation for this result is that Pb and Zn are present in the geochemistry fingerprint and not in the 'All' tracer fingerprint. Both of these elements were shown to be present in high concentrations in urban street dusts (Table 2), and have also been shown to be typically associated with larger particle size fractions in urban soils and sediment (Horowitz and Elrick 1987). Therefore, the selective deposition of only fine particles on the floodplain (as was

shown to occur in Figure 3), would cause the loss of large particles. The loss of Pb and Zn with these large particles would decrease the predicted contributions from urban street dusts made by the geochemistry tracer group, which would increase the predicted contributed from channel banks.

The opposite trend to that found in the Earls Barton core was seen in the Stanwick floodplain core (Table 7F); as SSA increases so does the predicted contribution made by the Geochem litho tracer group in relation to the 'All' tracer group. Likewise, in the Upton floodplain core the geochemistry group predicts increased contributions from channel banks in comparison to the 'All' tracer group as sediment SSA increases. In both of these cores the 'All' tracer group contains mineral magnetic signatures while the other tracer groups do not. In the published literature a positive relationship between geochemical tracers and SSA has been shown to commonly occur (Koiter et al. 2013) while the relationships with mineral magnetic signatures have been shown to be far more complex (Foster et al. 1998; Oldfield et al. 2009). Therefore, a potential interpretation of this result is that an increase in sediment SSA is resulting in a linear increase in geochemical tracer concentration in the core, changing the sediment provenance prediction. As shown by Foster et al. (1998) and Oldfield et al. (2009) magnetic signatures are likely not to follow the same positive linear relationship, resulting in a discrepancy in the predictions made by magnetic minerals and other tracers. However, it has been shown by Russell et al. (2001) that many tracers other than mineral magnetism can exhibit non-linear relationships with SSA; so tracer behaviour in reality is likely to be more complex than this generalisation.

The complexity of the relationships between tracers and SSA are demonstrated by the ineffectiveness of the particle size correction (see online supplementary table 4). The correction was used on the Earls Barton core with both tracer groups. A loss of tracer discriminatory efficiency occurred when the particle size correction was applied to the

Geochem litho group, which meant the correction could not be tested. However, the correction could be applied to the 'All' group. The correction resulted in a similar downcore trend to the uncorrected fingerprint but had less uncertainty associated with its prediction. The correction reduced the uncertainty produced by the Geochem and Geochem litho group in the Upton and Stanwick cores respectively, but did not change their down-core trends. The correction does however reverse the down-core trend of the 'All' tracer group in the Stanwick floodplain core.

4.4.3. *Alterations to geochemical and mineral magnetic signatures*

Mineral magnetic signatures have been shown to be affected by numerous processes which can cause the loss or alteration of specific sized magnetic grains. For example, smaller magnetic grains are preferentially dissolved before larger grains (Karlin and Levi 1983) causing a reduction in the concentration of magnetic signatures which account for small grains (χlf, χfd and χarm), in relation to signatures which also account for larger grains (SIRM and HIRM) (Anderson and Rippey 1988). The opposite trend of disproportionally low SIRM and HIRM concentrations in relation to χlf and χarm would be indicative of the loss of larger grains, through a process of selective transport. Only the non-conservatism of mineral magnetic signatures was directly investigated, due to their potential to indicate the loss of specific grain sizes; however the diagenesis of geochemical tracers has been shown to occur (Mayer et al. 1982). Therefore, the processes causing the dissolution of magnetic iron oxides would also be expected to impact geochemical and radionuclide tracers.

In the source samples there is a strong relationship between χlf and SIRM (Spearman rank p = 0.000, r = 0.913) (Figure 5A). Therefore, a change in sediment source is unlikely to alter the ratio between these two signatures and this ratio can be confidently used as an indicator of the non-conservatism of magnetic signatures. The relationship between χarm and SIRM is also

strongly linear for channel bank and surface agricultural source samples; however the urban street dust samples do not follow this relationship. Therefore, the results derived using this ratio should be carefully interpreted where a large proportion of urban sediment is likely to be present.

The χarm/ SIRM ratio in the Sywell reservoir core exceeded a value of 2 in the majority of core slices, indicating the likely in-growth of bacterial magnetite (Foster et al. 2008) (Table 6A). χarm is sensitive to the presence of bacterially produced stable single domain magnetite (Oldfield 2007), explaining why this tracer failed the mass conservation test (Table 3). The impact of this in-growth in Sywell reservoir is seen in the form of a positive correlation between χarm / SIRM and four of the differences between tracer group predictions (Table 6A).

In the Kingsthorpe and Stanwick floodplain cores (Table 6C; F), most differences between tracer group predictions were significantly correlated with χarm / SIRM, and with SIRM / χlf. Correlation coefficients ranged from 0.46 to 0.8 and 0.43 to 0.9 respectively, indicating that alterations to magnetic minerals are potentially an important process affecting tracers in this core. When χarm / SIRM increased and SIRM / χlf decreased, the predicted contribution from channel banks made by mineral magnetic signatures decreased. These results indicate that when a greater proportion of large remanence carrying magnetic grains were present in relation to small grains, mineral magnetic tracers predicted a greater contribution from channel banks. Channel banks are characterised by low magnetic signatures (Table 1), therefore the loss of magnetic grains through non-conservatism would cause an increased predicted contribution from this source. It is therefore possible that the dissolution of small magnetic grains in the deposited sediment is increasing the predicted contributions from channel banks made by magnetic signatures. The gleying of waterlogged floodplain sediments would result in such a loss of the mineral magnetic signatures and geochemical and lithogenic radionuclide tracers associated with iron oxides, and may be occurring in the Kingsthorpe core (Dearing et al. 1985)

As the sediments SSA in the Stanwick core is ~50% higher than the sediment source samples (Figure 3), the process of selective deposition of only fine magnetic grains is the most probable explanation for the discrepancy between tracer group predictions in this core.

The magnetic ratios were not significantly correlated with the large differences in tracer group predictions in the Upton floodplain core (Table 6D). However, all magnetic mineral tracers failed the range test in the Earls Barton core and the bottom half of the Upton core (which was not included in this section of the analysis). The floodplain in both of these coring locations was observed to be waterlogged, with much of each core having a blue tinted gleyed appearance, suggesting that the magnetic minerals were significantly affected by dissolution. The unrealistic 100% contribution of sediment from channel banks predicted by magnetic signatures in the Upton core probably reflects this process (Fig. 4E). Chemical processes such as gleying has been shown to alter magnetic signatures and to have similar effects on other tracer types. For example, wetting and drying cycles were shown to lead to elevated phosphorus release from floodplain sediments, which was related to enhanced reduction of iron hydroxides (Schönbrunner *et al.* 2012), supporting the relative stability of the sediments in the constantly wet Sywell reservoir in comparison to the floodplain cores. The rate at which different chemical elements are leached has also been shown to vary with Ca^{2+}, Na^+, K^+, Fe^{2+} and Mg^{2+} being selectively leached relative to relatively immobile hydrolysate constituents Al^{3+} and Ti^{4+} (Roy *et al.*, 2006)

The elements which can be present as radionuclides, such as K and U, have been shown to have a high mobility in the environment when compared to the largely immobile elements such as Th, Ac, Ra and Pb (Balonov *et al* (2010). For example, ^{226}Ra has been shown to be mobilised by groundwater resulting in an enrichment in lake and wetland sediment (Brenner *et al.* 2004). Plant uptake and the biogeochemical cycling of chemical elements is also a key process which can alter tracers, especially when utilising tracers in sediment on a floodplain where vegetation grows on deposited sediment. For example Papastefanou *et al.* (2005)

showed that half of the ^{137}Cs Chernobyl fallout was being cycled through plants 40 months after its fallout.

In addition to dissolution and in-growth effects Lees (1997) showed that errors of up to 2% could occur with susceptibility measurements, and up to 16% with remanence measurements due to a lack of linear additivity. In the Nene, contrasts in median mineral magnetic signatures in the source groups ranged from 30% (HIRM) up to 214% (χfd) (Table 2). Therefore significant errors to predictions made using HIRM could be caused through non-linear additivity effects.

4.5. Limitations

Differences in catchment lithology could potentially be driving the differences between tracer group predictions found in the Nene basin. The soils on ironstone and limestone contained significantly different tracer concentrations to the diamicton, clays and silts. Therefore, variation in inputs from different lithologies could be increasing the discussed spatial variability effects. Discrimination between subsurface and surface sediment sources may also be a result of differences in lithology, therefore, unless an amount of sediment was contributed from each lithology in proportion to its representation in the source samples the basis for source discrimination may be lost for many tracers.

Alterations to tracer signatures over historical timescales may also represent an unaccounted for source of uncertainty. For example, changes in traffic density and industrial pollutant emissions are likely to have changed tracer concentrations in road dusts, and in surface soils due to atmospheric fallout. Therefore, the composite signatures derived using present day source samples may not be able to discriminate between sediment sources over historical timescales.

Land use on the floodplain samples could also have altered the tracer signatures. While it was established that the sites had not been cultivated, the sites were observed to have been grazed

by livestock, which may have altered tracer signatures by the removal of tracers with consumed vegetation, inputs of excrement containing tracers or the mechanical disturbance of the deposited sediment.

4.6.   Recommendations

The findings of this study have highlighted the importance of accounting for particle size, organic matter and diagenetic related changes to tracer signatures. Developing specific relationships between tracer signatures, particle size and organic matter may be a potential way to accurately determine sediment provenance in the Nene and similar catchments elsewhere. Methodologies such as that used by Motha *et al* (2003) have successfully incorporated such an approach, yet subsequent research has rarely implemented it. The fractionation of sediment and sources into narrower particle size bands than the <63 μm fraction present less labour intensive potential methods to mitigate particle size effects. Such a method has been used by Laceby and Olley, (2014) who limited analysis to the <10 μm fraction and particle size specific tracing has been used by Hatfield and Maher (2009).

Additional methodological improvements which may improve the accuracy of future research include the use of artificially generated mixtures of tracer signatures, which have been previously used by Haddadchi et al. (2014) and Lees (1997). Such approaches could be used to assess the potential impacts of spatial variability or changing sediment particle size and organic matter content. The robust basis for source discrimination provided by differences in lithology could also be more extensively utilised to assess geological inputs, minimise the potential for tracer signatures to have changed over historical timescales and potentially maximise the contrasts in tracer signatures of the source groups.

5. Conclusions

The successful use of fingerprinting in Sywell reservoir shows the potential for the fingerprinting of historically deposited lake sediments to reconstruct past changes to the fluvial environment. For the other cores had any of the tracer groups been used in isolation, a prediction of sediment provenance would have been derived using a composite fingerprint able to differentiate between the source groups, and an acceptable goodness of fit would have been established, indicating that the fingerprinting had been successful. However, the different provenance predictions and down-core trends produced when using the different tracer groups suggests that the fingerprints are not consistently reflecting sediment provenance.

The implication of this result is that when fingerprinting is undertaken in environments similar to Nene basin, where the preservation of signatures is poor, alterations to tracer signatures must be investigated and mitigated for within the fingerprinting methodology. It must be concluded that for many of the cores investigated the fingerprinting method used did not determine the sediment provenance within an acceptable degree of uncertainty and that an improved methodology would be required to obtain this data.

When considering alterations to tracer signatures it was found that the organic content of the sediment was significantly correlated with an increase in the differences between tracer group predictions in the Sywell reservoir, as well as the Kingsthorpe, Upton and Stanwick floodplain cores. The particle size of the sediment was significantly correlated with the differences between most tracer group predictions in the Upton, Earls Barton and Stanwick floodplain cores. The findings of this paper therefore indicate that these commonly cited reasons for tracer non-conservatism are likely to be major factors causing uncertainty when fingerprinting sediment with a highly different organic matter content or particle size to the potential source samples. The simple corrections for particle size and organic matter were generally ineffective at reducing the differences between tracer group predictions, suggesting that relationships between tracers, organic matter and particle size are more complex than the

corrections assume. Consideration should also be directed to the findings of Pulley *et al.* (2015) who showed that uncertainties could originate from an insufficient contrast between tracer groups before tracer conservatism is even considered. The close agreement between tracer groups when fingerprinting the highly distinctive urban road dust source in this study supports this finding, and further suggests that the effects of tracer non-conservatism are reduced when large contrasts in tracer signatures exist between sediment sources.

References

Anderson NJ, Rippey B (1988) Diagenesis of magnetic minerals in the recent sediments of a eutrophic lake. Limnol Oceanogr 33:1476–1492

Balonov M, Barnett CL, Belli M, Beresford NA, Berkovsky V, Bossew P, Boyer P, Brittain JE, Calmon P, Carini F, Choi YH, Ciffroy P, Colle C, Conney S, Davis P, Durrieu G, Ehlken S, Fesenko S, Galeriu DC, Garcia-Sanchez L, Garnier JM, Gerzabek MH, Gil-García CJ, Golikov V, Gondin Fonseca AM, Howard, BJ, Hubmer A, Isamov N, Jourdain F, Jova Sed L, Juri Ayub J, Kashparov V, Kirchner G, Krasnov V, Leclerc E, Lettner H, Linsley G, Louvat D, Madoz-Escande C, Martin P, Melintescu A, Monte L, Olyslaegers G, Orlov O, Palsson SE, Periañez R, Peterson SR, Pröhl G, Rantavaara A, Ravi PM, Reed E, Rigol A, Sansone U, Sanzharova N, Saxén R, Shang ZR, Shaw G, Shubina O, Siclet F, Skuterud L, Smith JT, Strebl F, Tagami K, Tamponnet C, Thiry Y, Uchida S, Vandenhove H, Varga B, Velasco H, Vidal M, Voigt G, Yankovich T, Zeiller L, Zibold G (2010) *Handbook of Parameter Values for the Prediction of Radionuclide Transfer in Terrestrial and Freshwater Environment.* Austria, IAEA, 194. Technical Reports Series, 472.

Bihari Á, Dezső Z (2007) Examination of the effect of particle size on the radionuclide content of soils. J Environ Radioactiv 99(7):1083-1089. DOI: 10.1016/j.jenvrad.12.020

Caitcheon G (1993) Sediment source tracing using environmental magnetism: A new approach with examples from Australia. Hydrol Process 7(4):349-358. DOI: 10.1002/hyp.3360070402

Carter J, Owens PN, Walling DE, Leeks GJL (2003) Fingerprinting suspended sediment sources in a large urban river system. Sci Total Environ 314–316:513-534. DOI: 10.1016/S0048-9697(03)00071-8

Charlesworth SM, Foster IDL (2005) Gamma emitting radionuclides and heavy metals in urban dusts and sediments, Coventry, UK: implications of dosages for dispersal and disposal. Mineralogical Magazine 69:759-767. DOI: 10.1180/0026461056950286

Charlesworth S, Everett M, McCarthy R, Ordo´n˜ez, A, de Miguel E (2003) A comparative study of heavy metal concentration and distribution in deposited street dusts in a large and a small urban area: Birmingham and Coventry, West Midlands, UK, Environ Int 29:563– 573. DOI: 10.1016/S0160-4120(03)00015-1

Collins AL, Walling DE, Stroud RW, Robson M, Peet LM (2010a) Assessing damaged road verges as a suspended sediment source in the Hampshire Avon catchment, southern United Kingdom. Hydrol Process 24(9):1106-1122. DOI: 10.1002/hyp.7573.

Collins AL, Walling DE, Leeks GJL (1997a) Source type ascription for fluvial suspended sediment based on a quantitative composite fingerprinting technique. Catena 29(1): 1-27. DOI: 10.1016/S0341-8162(96)00064-1

Collins AL, Walling DE, Leeks GJL (1997b) Use of the geochemical record preserved in floodplain deposits to reconstruct recent changes in river basin sediment sources. Geomorphology 19(1–2):151-167. DOI: 10.1016/S0169-555X(96)00044-X

Collins AL, Walling DE, Stroud RW, Robson M, Peet LM (2010a) Assessing damaged road verges as a suspended sediment source in the Hampshire Avon catchment, southern United Kingdom. Hydrol. Process. 24(9), 1106-1122.

Collins AL, Walling DE, Webb L, King P (2010b) Apportioning catchment scale sediment sources using a modified composite fingerprinting technique incorporating property weightings and prior information, Geoderma 155(3–4):249-261. DOI: 10.1016/j.geoderma.2009.12.008

Davis RJ, Gregory KJ (1994) A new distinct mechanism of river bank erosion in a forested catchment. J Hydrol 157(1–4): 1-11. DOI: 10.1016/0022-1694(94)90095-7

Dearing JA, Maher B, Oldfield F (1985) Geomorphological linkages between soils and sediments: the role of magnetic measurements. In: Richards K (ed) Geomorphology and Soils, Allen & Unwin, London, pp 245 – 266

Foster IDL (2006) Lakes in the Sediment Delivery System. In: Owens PN, Collins, AJ (Eds) Soil Erosion and Sediment Redistribution in River Catchments. Wallingford, CAB International. 128-142. DOI: 10.1079/9780851990507.0128

Foster IDL (2010) Lakes and reservoirs in the sediment cascade. In: Burt TP, Allison RJ (eds) Editors. Sediment Cascades: an Integrated Approach, Wiley, Chichester UK, pp 345-376

Foster IDL, Lees JA (2000) Tracers in geomorphology: Theory and applications in tracing fine particulate sediments. In: Foster IDL (ed) Tracers in Geomorphology, Wiley Chichester UK, pp 3-20.

Foster IDL, Walling DE (1994) Using reservoir deposits to reconstruct changing sediment yields and sources in the catchment of the Old Mill Reservoir, South Devon, UK, over the past 50 years. Hydrolog Sci J 39:347-368.

Foster IDL, Boardman J, Keay-bright J, Meadows M E (2005) Land degradation and sediment dynamics in the South African Karoo. In: Horowitz AJ, Walling DE (2005) Proceedings of symposium S1 held during the 7th IAHS Scientific Assembly in April 2005, Brazil.

Foster IDL, Lees JA, Owens PN, Walling DE (1998) Mineral magnetic characterization of sediment sources from an analysis of lake and floodplain sediments in the catchments of the Old Mill reservoir and Slapton Ley, South Devon, UK. Earth Surf Proc Land 23(8):685-703. DOI: 10.1002/(SICI)1096-9837(199808)23:8<685:AID-ESP873>3.0.CO;2-8

Foster IDL, Boardman J, Keay-Bright J (2007) Sediment tracing and environmental history for two small catchments, Karoo Uplands, South Africa. Geomorphology 90(1–2):126-143. DOI: j.geomorph.2007.01.011

Foster IDL, Oldfield F, Flower RJ, Keatings K (2008) Mineral magnetic signatures in a long core from Lake Qarun, Middle Egypt. J Paleolim 40(3):835-849. DOI: 10.1007/s10933-008-9202-x

Foster IDL, Rowntree KM, Boardman J, Mighall TM (2012) Changing sediment yield and sediment dynamics in the Karoo uplands, South Africa; post-European impacts. Land Degrad Dev 23(6):508-522. DOI: 10.1002/ldr.2180

Gray AB, Pasternack GB, Watson EB (2010) Hydrogen peroxide treatment effects on the particle size distribution of alluvial and marsh sediments. The Holocene 20(2):293-301

Gruszowski KE (2003) Erosion, sediment yields, sediment sources, storage and transport pathways in the catchment of the River Leadon Herefordshire, UK. University of Coventry, UK: PhD thesis

Haddadchi A, Olley J, Laceby P (2014) Accuracy of mixing models in predicting sediment source contributions. Science of The Total Environment 497 – 498: 139 – 152. DOI: 10.1016/j.scitotenv.2014.07.105

Hatfield RG, Maher BA (2009) Fingerprinting upland sediment sources: particle size-specific magnetic linkages between soils, lake sediments and suspended sediments. Earth Surf Proc Land 34(10): 1359–1373 DOI: 10.1002/esp.1824

Hirner AV, Kritsotakis K, Tobschall HJ (1990) Metal-organic associations in sediments—I. Comparison of unpolluted recent and ancient sediments and sediments affected by anthropogenic pollution. Appl Geochem 5(4):491-505. DOI: 10.1016/0883-2927(90)90023-X

Heiri O, Lotter AF, Lemcke G (2001) Loss on ignition as a method for estimating organic and carbonate content in sediments, reproducibility and comparability of results. J Paleolim 25:101–110. DOI: A:1008119611481

Horowitz AJ (1991) A primer on sediment-trace element chemistry, 2nd edition, Lewis Publishers, USA

Horowitz AJ, Elrick KA (1987) The relation of stream sediment surface area, grain size and composition to trace element chemistry. Appl Geochem 2:437-451. DOI: 10.1016/0883-2927(87)90027-8

Karlin R, Levi S (1983) Diagenesis of magnetic minerals in recent hemipelagic sediments. Nature 303:327–330

Klages MG, Hsieh YP (1975) Suspended Solids Carried by the Gallatin River of Southwestern Montana: II. Using Mineralogy for Inferring Sources. J Environ Qual 4:68-73. DOI: 10.2134/jeq1975.00472425000400010016x

Koiter AJ, Owens PN, Petticrew EL, Lobb DA (2013) The behavioural characteristics of sediment properties and their implications for sediment fingerprinting as an approach for identifying sediment sources in river basins. Earth-Sci Rev 125:24-42. DOI: 10.1016/j.earscirev.2013.05.009

Krein A. Petticrew E. Udelhoven T (2003) The use of fine sediment fractal dimensions and colour to determine sediment sources in a small watershed. Catena 53:165-179. DOI: 10.1016/S0341-8162(03)00021-3

Laceby JP, Olley J (2014) An examination of geochemical modelling approaches to tracing sediment sources incorporating distribution mixing and elemental correlations. Hydrol. Process In Press. DOI: 10.1002/hyp.10287

Lees J (1999) Evaluating magnetic parameters for use in source identification, classification and modelling of natural and environmental materials. In: Walden J, Oldfield F, Smith J (eds) Environmental magnetism, a practical guide. Technical Guide No. 6, Quaternary Research Association, London, pp 113-138

Lees JA (1997) Mineral magnetic properties of mixtures of environmental and synthetic materials: linear additivity and interaction effects. Geophys J Int 131(2):335-346.

Mackereth FJH (1969) A short core sampler for sub-aqueous deposits. Limnol Oceanogr 14:145-151. DOI:10.4319/lo.1969.14.1.0145

Mayer LM, Liotta FP, Norton SA (1982) Hypolimnetic redox and phosphorus cycling in hypcreutrophic lake Sebasticook, Maine. Water Res 16:1189-1196.

Miller JR, Lord M, Yurkovich S, Mackin G, Kolenbrander L (2005) Historical trends in sedimentation rates and sediment provenance, Fairfield lake, western North Carolina. J Am Water Resour As 41(5):1053-1075. DOI: 10.1111/j.1752-1688.2005.tb03785.x

Morton RD, Rowland C, Wood C, Meek L, Marston C, Smith G, Wadsworth R, Simpson I (2011) Land Cover Map 2007 (Vector, GB). NERC-Environmental Information Data Centre. DOI:10.5285/1d78e01a-a9c1-4371-8482-1c1b57d9661f.

Motha JA, Wallbrink PJ, Hairsine PB, Grayson RB (2003) Determining the sources of suspended sediment in a forested catchment in southeastern Australia. WATER RESOUR RES 39(3):1056. DOI: 10.1029/2001WR000794

Nadeu E, Vente J, MartÃnez-Mena M, Boix-Fayos C (2011) Exploring particle size distribution and organic carbon pools mobilized by different erosion processes at the catchment scale. J Soils Sediments 11(4):667-678. DOI: 10.1007/s11368-011-0348-1

Oldfield F, Barnosky C, Leopold EB, Smith JP (1983) Mineral magnetic studies of lake sediments. Hydrobiologia 103(1):37-44. DOI: 10.1007/BF00028425.

Oldfield F (2007) Sources of fine-grained magnetic minerals in sediments: a problem revisited. The Holocene 17: 1265–1271. DOI: 10.1177/0959683607085135

Oldfield F, Hao Q, Bloemendal J, Gibbs-Eggar Z, Patil S, Guo Z (2009) Links between bulk sediment particle size and magnetic grain-size: general observations and implications for Chinese loess studies. Sedimentology 56(7):2091-2106. DOI: 10.1111/j.1365-3091.2009.01071.x

Owens PN, Walling DE, Leeks GJL (1999) Use of floodplain sediment cores to investigate recent historical changes in overbank sedimentation rates and sediment sources in the catchment of the River Ouse, Yorkshire, UK. *Catena* 36(1–2), 21-47. DOI: 10.1016/S0341-8162(99)00010-7

Pittam NJ, Foster IDL, Mighall TM (2008) An integrated lake-catchment approach for determining sediment source changes at Aqualate Mere, Central England. J Paleolim. 42(2), 215-232. DOI: 10.1007/s10933-008-9272-9

Pulley SJ, Foster IDL, Antunes P (2015) The uncertainties associated with sediment fingerprinting suspended and recently deposited fluvial sediment in the Nene river basin. Geomorphology **228**: 303-319. DOI: 10.1016/j.geomorph.2014.09.016

Russell MA, Walling DE, Hodgkinson RA (2001) Suspended sediment sources in two small lowland agricultural catchments in the UK. J Hydrol 252(1–4):1-24. DOI: 10.1016/S0022-1694(01)00388-2

Schönbrunner IM, Preiner S, Hein T (2012) Impact of drying and re-flooding of sediment on phosphorus dynamics of river–floodplain systems. Sci Total Environ **432**, 329–337 DOI:10.1016/j.scitotenv.2012.06.025

Smith J, Beresford NA (2005) Chernobyl: Catastrophe and consequences. Berlin: Springer

Stamp LD (1932) The Land Utilisation Survey of Britain. Nature 129: 709-711

Swanson V. Frist L. Rader R Jr, Huffman C Jr (1966) Metal sorption by northwest Florida humate: U.S. Geological Survey Professional Paper 550-C; pp 174-177

Thompson R, Morton DJ (1979) Magnetic susceptibility and particle size distribution in recent sediments of the Loch Lomond drainage basin Scotland. J Sediment Petrol 49(3):801-912. DOI:. 10.1306/212F7851-2B24-11D7-8648000102C1865D

Tsabaris C, Eleftueriou G, Kapsimalis V, Anagnostou C, Vlastou R, Durmishi C, Kedhi M, Kalfas CA (2007) Radioactivity levels of recent sediments in the Butrint Lagoon and the adjacent coast of Albania. Appl Radiat Isotopes 65:445-453. DOI: 10.1016/j.apradiso.2006.11.006

Walden J. Remanence Measurements (1999) In: Walden J, Oldfield F, Smith JP (eds) Environmental Magnetism A Practical Guide, Technical Guide No 6, Quaternary Research Association, London, pp 63-88.

Wallbrink PJ, Olley JM, Roddy BP (1997) Quantifying the redistribution of soils and sediments within a post-harvested forest coupe near Bombala, New South Wales, Australia: Technical Report 7/97

Wallbrink PJ, Walling DE, He Q (2003) Radionuclide Measurement Using HPGe Gamma Spectrometry. In: Zapata F (ed) Handbook for the Assessment of Soil Erosion and Sedimentation Using Environmental Radionuclides, Springer, Netherlands, pp 67-96. DOI: 10.1007/0-306-48054-9_5

Walling D, Webb B ,Shanahan J (2008) Investigations into the use of critical sediment yields for assessing and managing fine sediment inputs into freshwater ecosystems. Natural England Research Information Note RIN007. Natural England; www.naturalengland.org.uk

Walling DE (2013) The evolution of sediment source fingerprinting investigations in fluvial systems. J Soils Sediments 13(10):1658-1675. DOI 10.1007/s11368-013-0767-2

Wang Z, Govers G, Steegen A, Clymans W, Van den Putte A, Langhans C, Merckx R, Van Oost K (2010) Catchment-scale carbon redistribution and delivery by water erosion in an intensively cultivated area. Geomorphology 124(1–2):65-74. DOI: 10.1016/j.geomorph.2010.08.010

Winter LT, Foster IDL, Charlesworth SM, Lees JA (2001) Floodplain lakes as sinks for sediment-associated contaminants — a new source of proxy hydrological data? Sci Total Environ 266(1–3):187-194. DOI: 10.1016/S0048-9697(00)00745-2
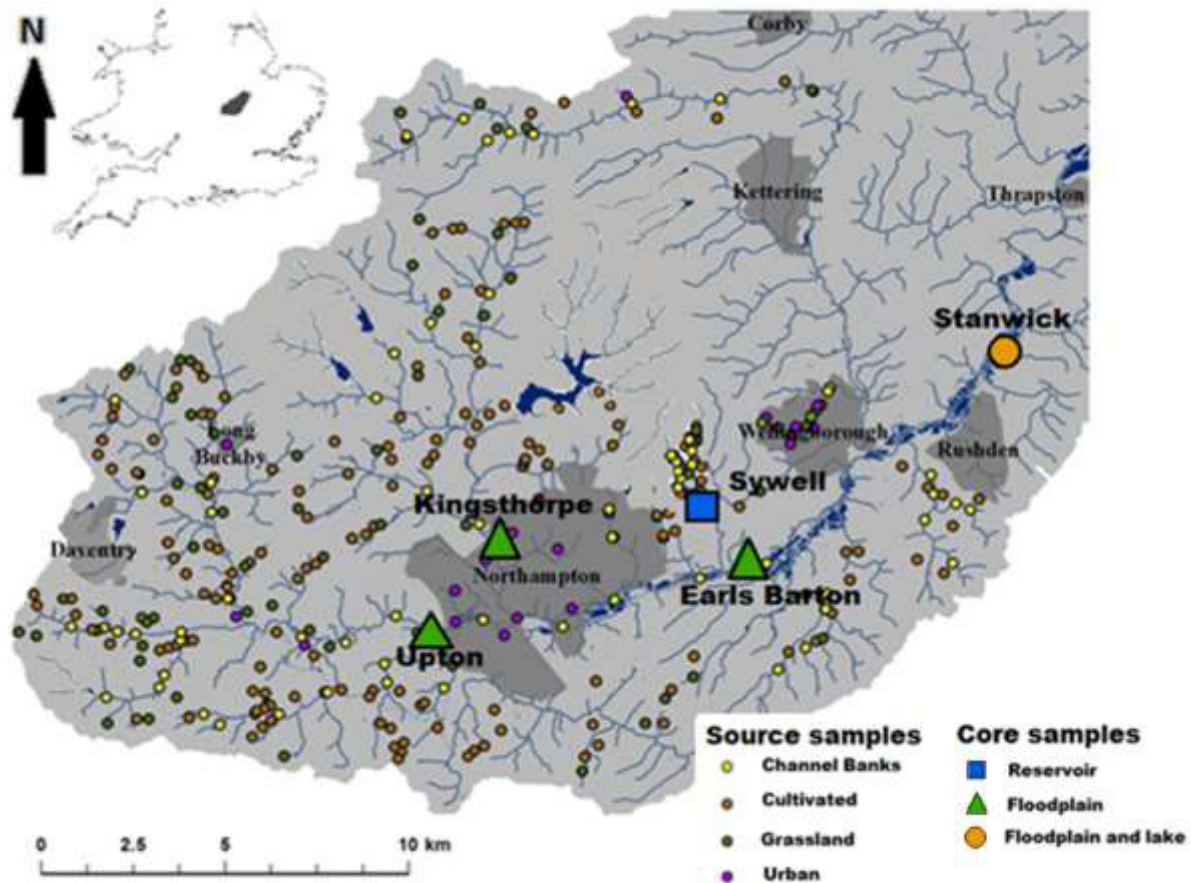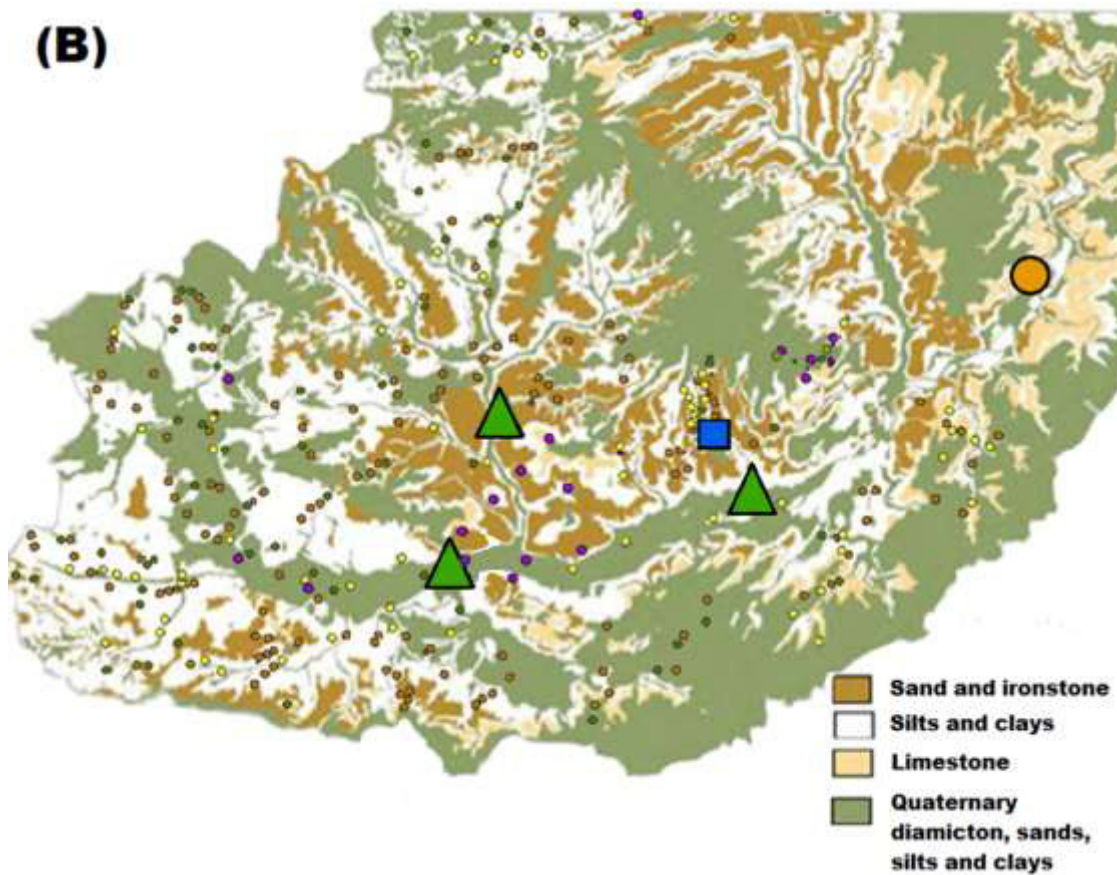
Figure 1: River Nene catchment with sampling locations (A) and catchment geology (B), Northampton located at 52°13'47.84"N 0°54'26.12"W, The white area represents

the area of the Nene basin and the grey shading shows the extent of major urban areas in the Nene catchment
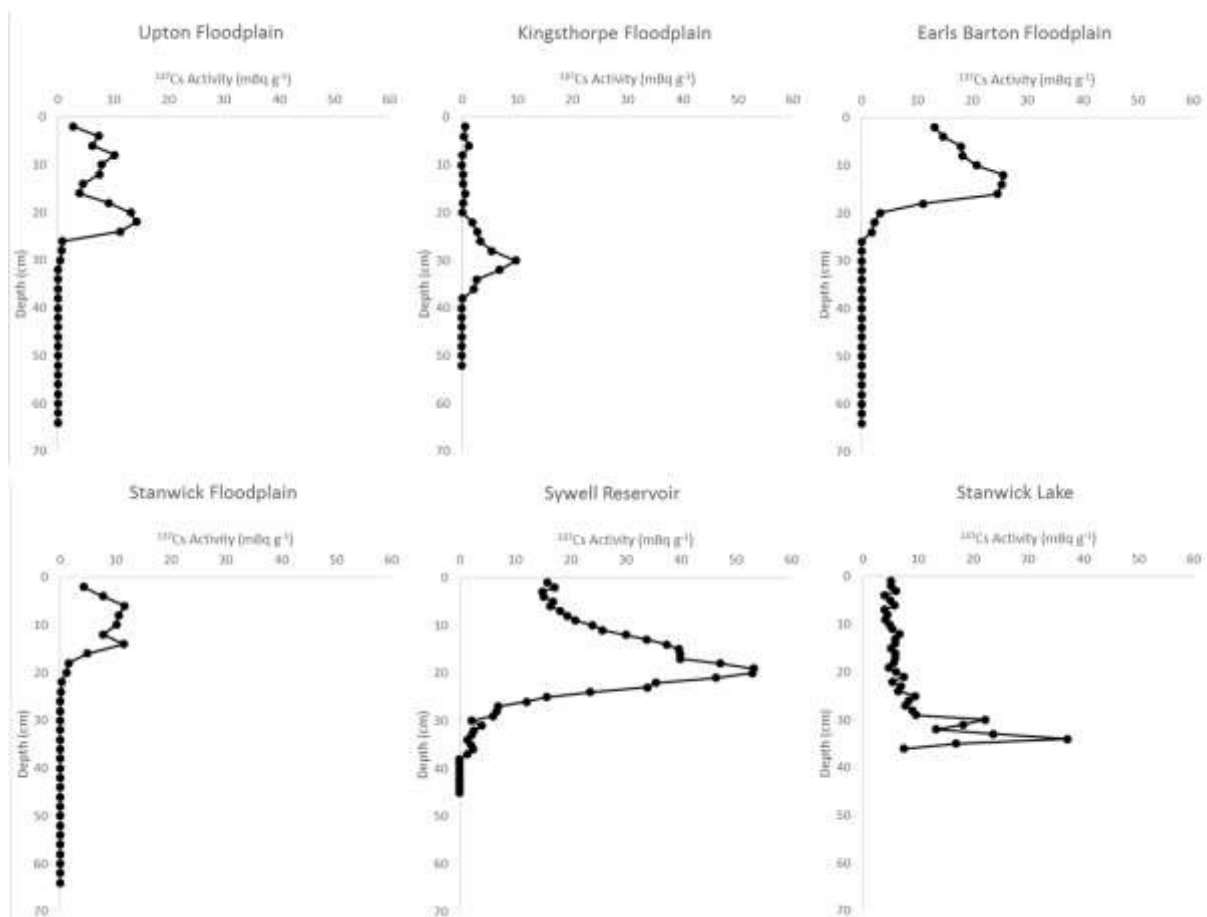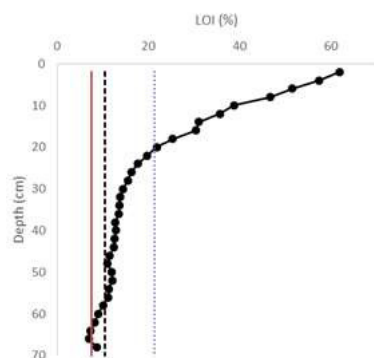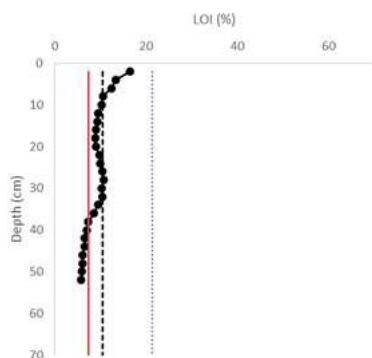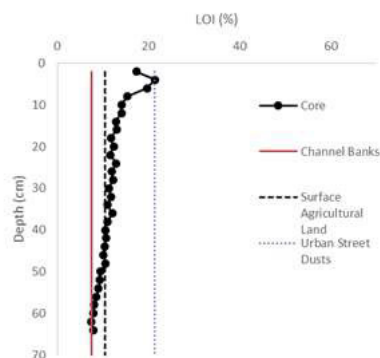
Figure 2: Down-core plots of ^{137}Cs activity in the lake and floodplain cores.

A

Earls Barton Floodplain · Kingsthorpe Floodplain · Stanwick Floodplain

Upton Floodplain · Sywell Reservoir · Stanwick Lake

Legend: Core · Channel Banks · Surface Agricultural Land · Urban Street Dusts

B

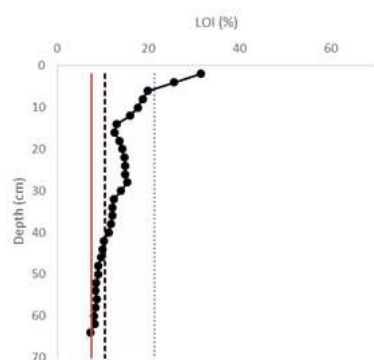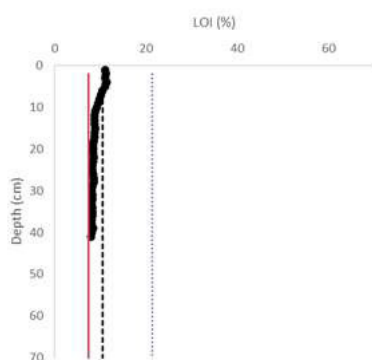Earls Barton Floodplain · Kingsthorpe Floodplain · Stanwick Floodplain

Upton Floodplain · Sywell Reservoir · Stanwick Lake

Legend: Core · Channel Banks · Surface Agricultural Land · Urban Street Dusts
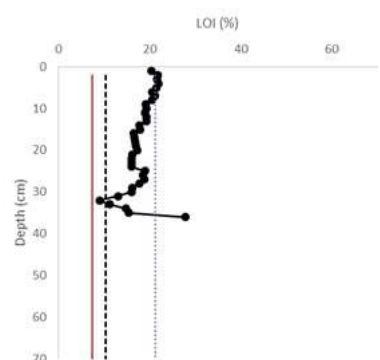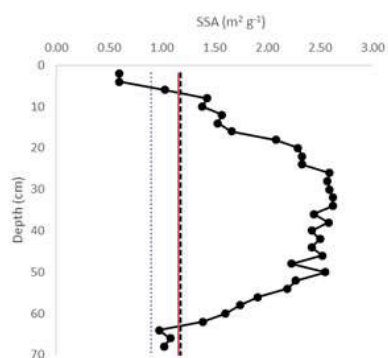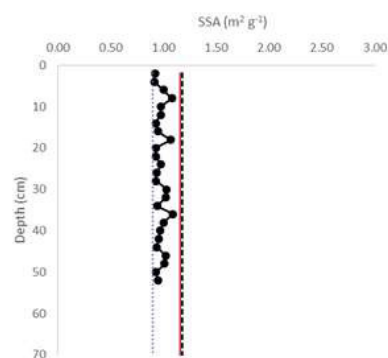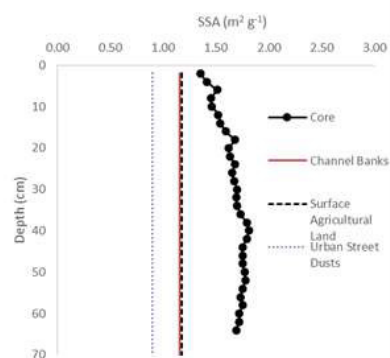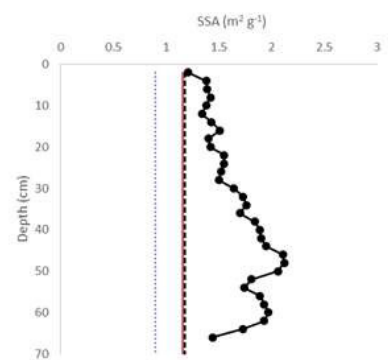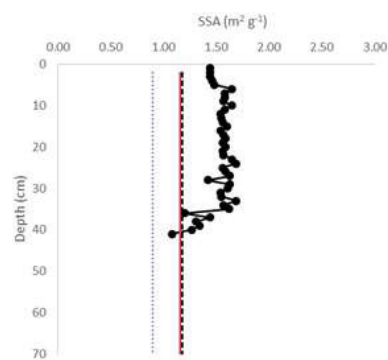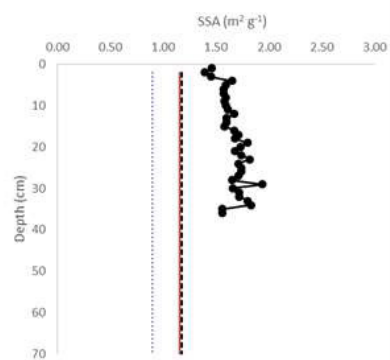
Figure 3: Down-core profiles of the LOI (A) and SSA (B) of the sediment cores.
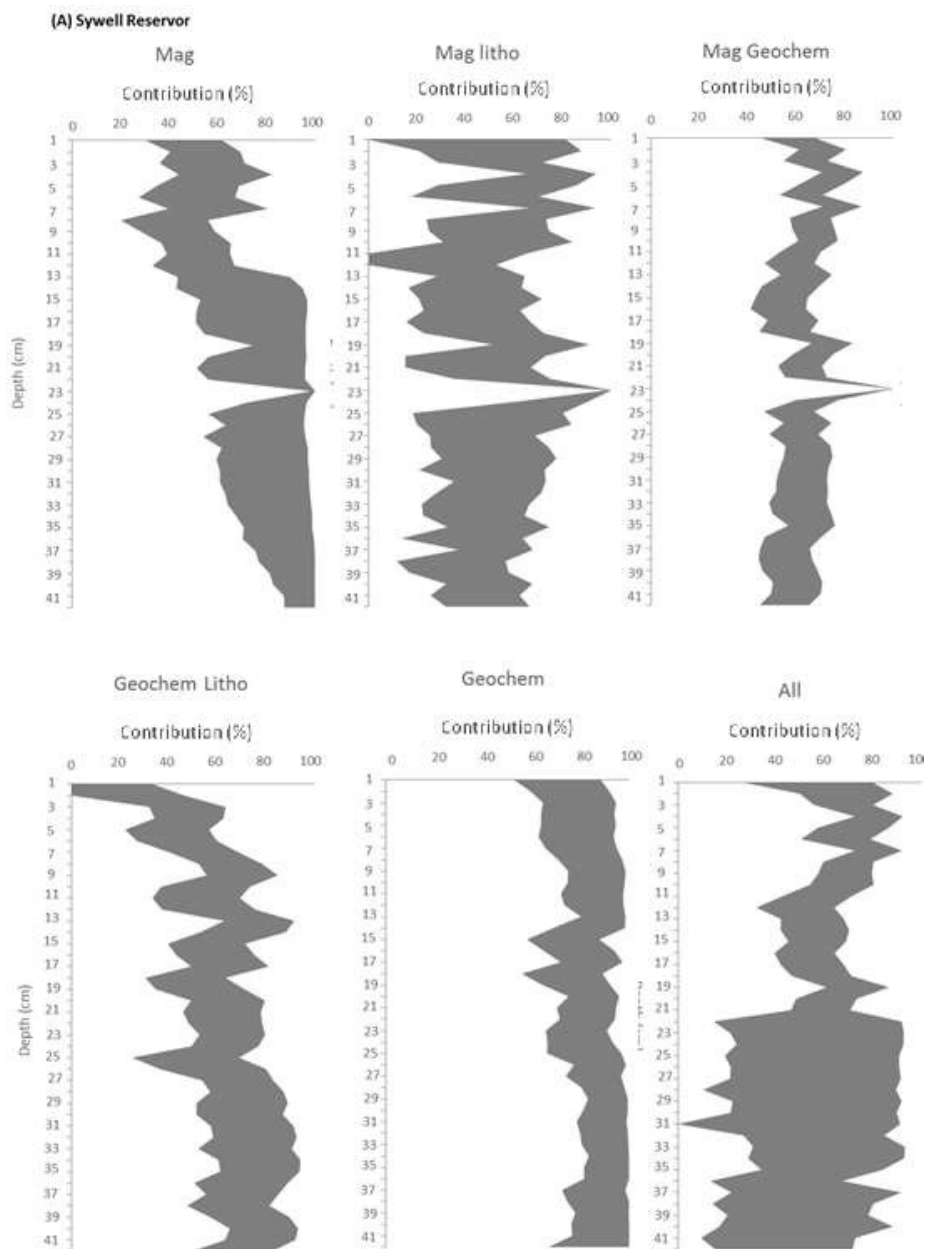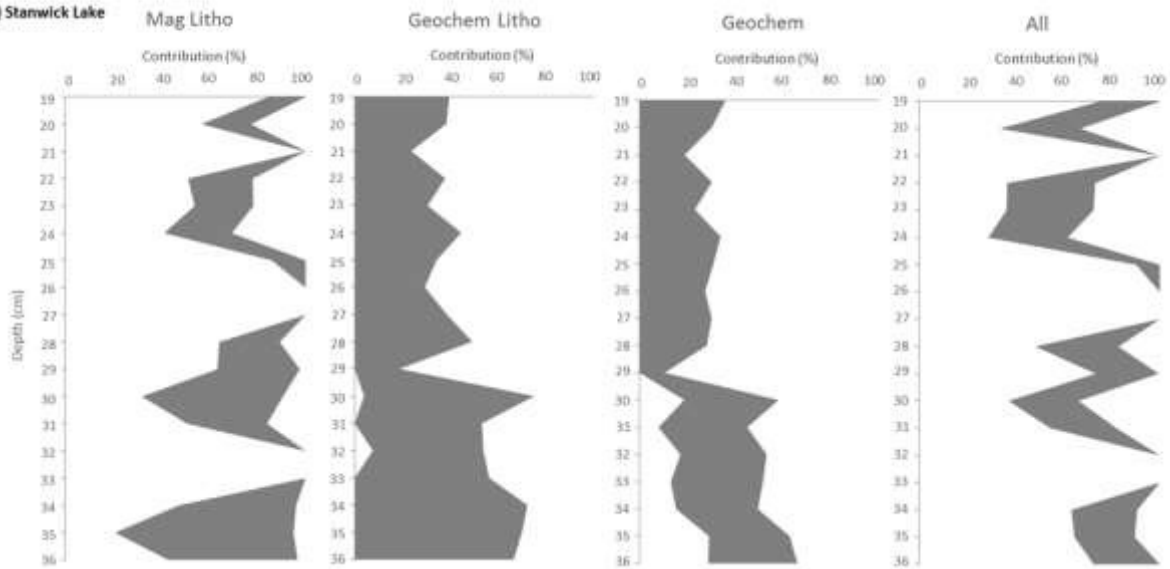
(A) Sywell Reservoir

(B) Stanwick Lake

Mag Litho Geochem Litho Geochem All

(C) Kingsthorpe Floodplain

Mag Mag Litho Mag Geochem Geochem Litho

Geochem All Geochem Fallout Mag Fallout
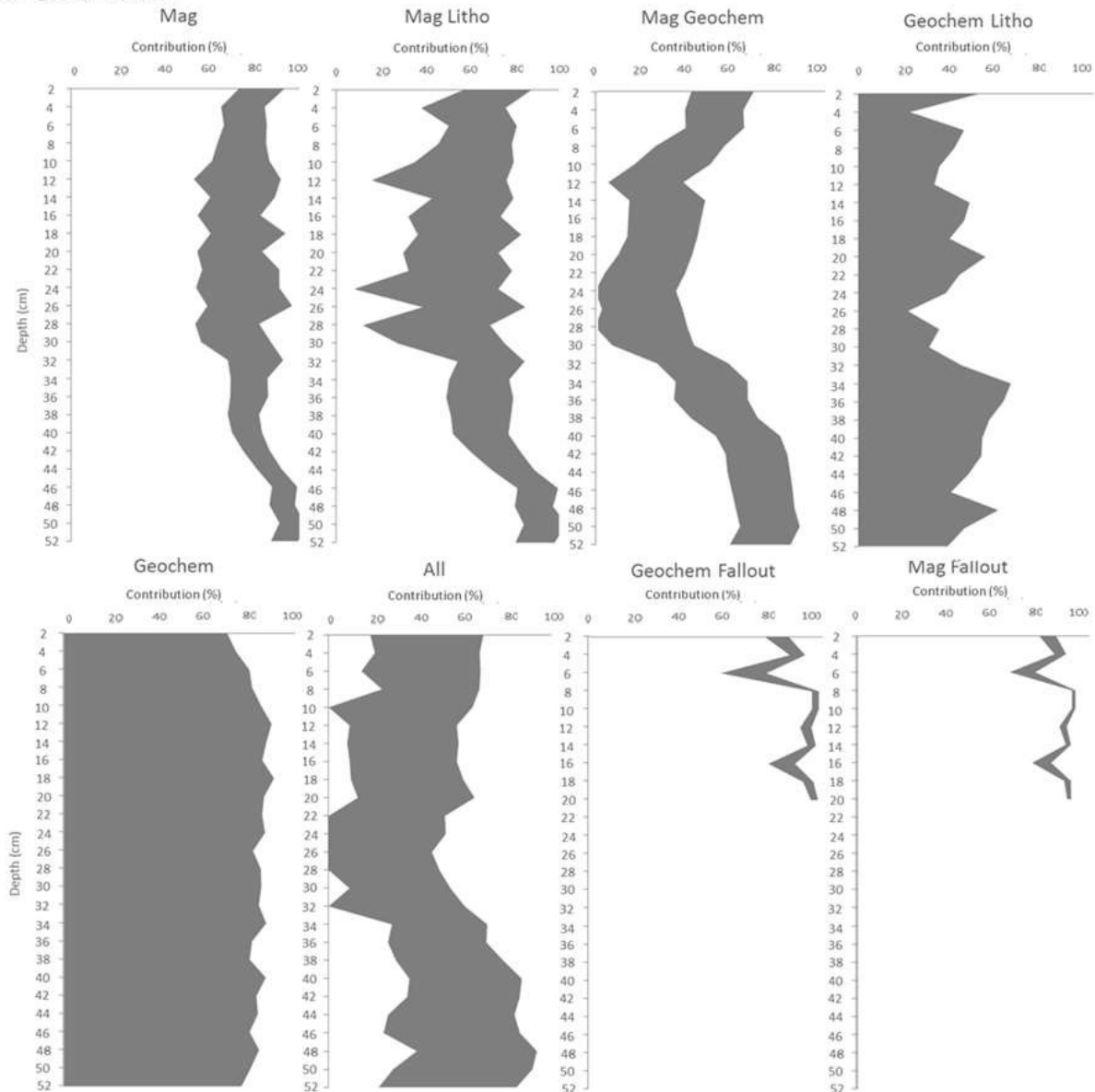
(D) Earls Barton Floodplain
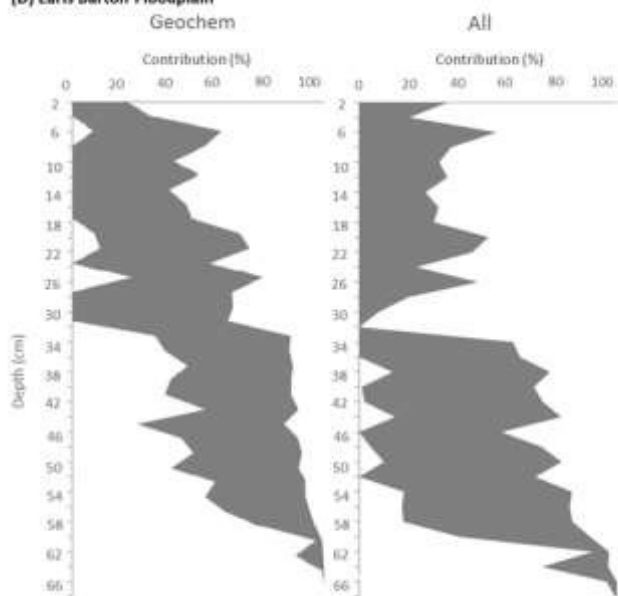
(E) Upton Floodplain
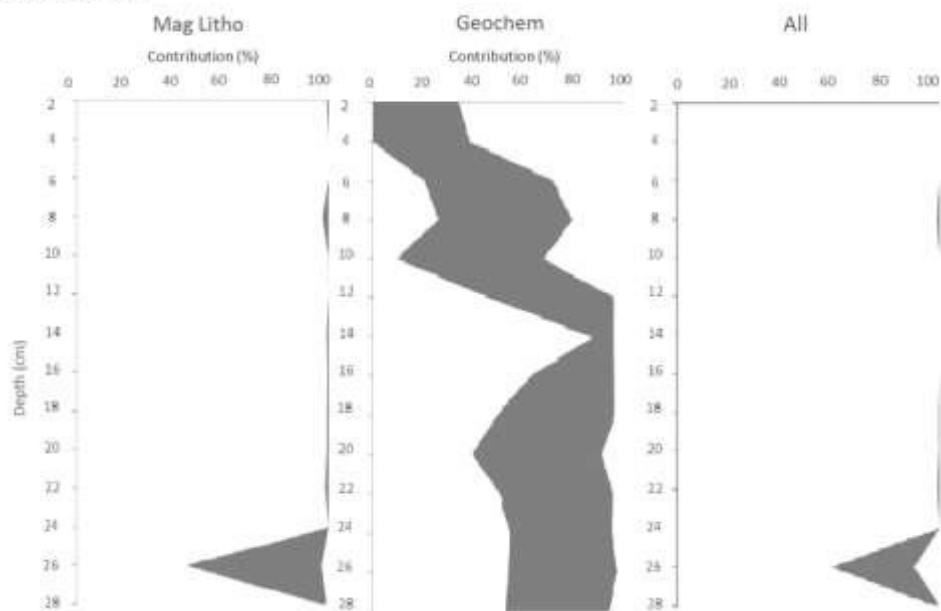
(F) Stanwick Floodplain
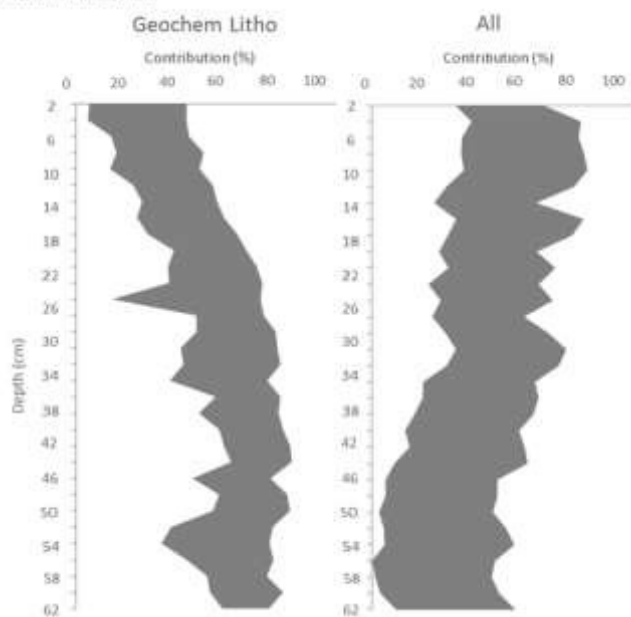
Figure 4: Down core plots of the median predicted contributions from channel banks derived using the different uncorrected tracer fingerprints and historically deposited sediment, the grey area represents the range between the 25th and 75th percentile predicted contributions.
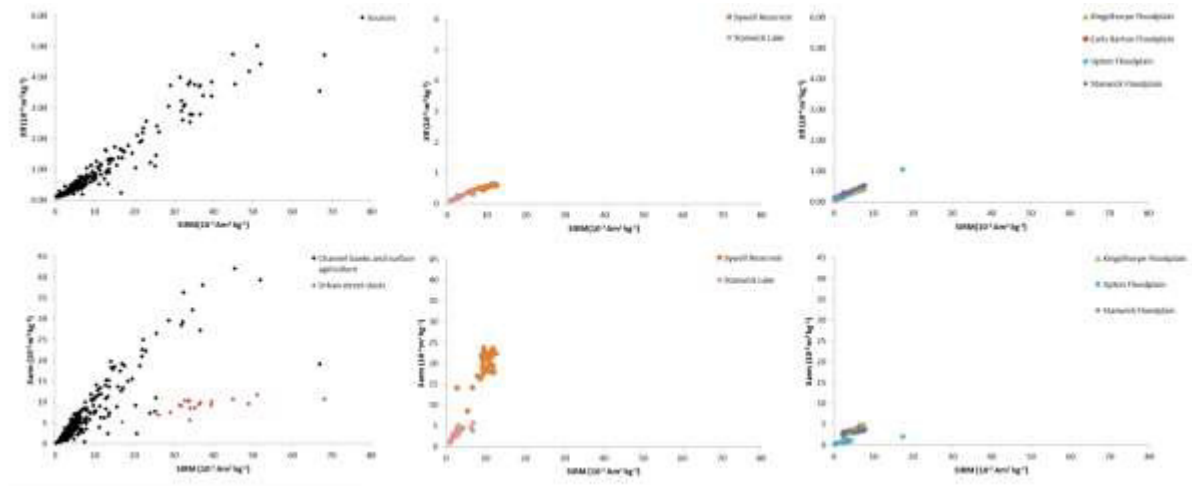
Figure 5: The relationships between χlf and SIRM (A), and χarm and SIRM (B) in sediment source samples.

Table 1: The tracer groups used to fingerprint historically deposited sediment and their abbreviations.

Tracer group fingerprint	Abbreviation
Mineral magnetic signatures	Mag
Mineral magnetics and lithogenic radionuclides	Mag litho
Mineral magnetics and geochemistry	Mag geochem
Geochemistry and lithogenic radionuclides	Geochem litho
Geochemistry	Geochem
All tracer groups combined.	All

Table 2: Median tracer concentrations in sediment source groups reported with median absolute deviations.

Source property	Surface Sources		Chanel Banks		Urban Street dusts	
	Median	Median absolute deviation	Median	Median absolute deviation	Median	Median absolute deviation
LOI (%)	10.44	1.23	7.47	1.03	21.34	2.57
SSA (m^2 g^{-1})	1.18	0.10	1.16	0.08	0.90	0.07
χ_{lf} (10^{-6} m^3 kg^{-1})	0.38	0.18	0.22	0.05	3.73	0.45
χ_{fd} (10^{-9} m^3 kg^{-1})	21.41	14.19	6.81	3.39	124.75	20.12
χarm (10^{-6} m^3 kg^{-1})	3.67	2.36	1.46	0.66	9.44	0.91
IRM1T (10^{-5} m^3 kg^{-1})	4.50	2.18	2.53	0.96	34.11	2.62
IRM$_{-100}$ (10^{-5} m^3 kg^{-1})	-3.49	1.85	-1.68	0.74	-25.98	3.08
HIRM (10^{-5} m^3 kg^{-1})	0.52	0.18	0.40	0.09	4.57	0.59
^{226}Ra (mBq g^{-1})	31.25	8.30	34.54	9.94	10.31	2.80
^{137}Cs (mBq g^{-1})	2.89	1.24	0.16	0.16	0.75	0.39
^{228}Ac (mBq g^{-1})	32.86	6.17	36.89	6.19	15.91	4.71
^{40}K (mBq g^{-1})	612.58	84.17	645.74	91.08	388.96	51.66
^{234}Th (mBq g^{-1})	20.27	5.55	18.16	4.90	6.79	1.28
^{235}U (mBq g^{-1})	2.28	0.96	2.23	0.95	0.93	0.28
^{212}Pb (mBq g^{-1})	34.25	6.05	38.40	5.33	19.89	2.18
Al (mg kg^{-1})	9488	1463	8841	1974	11868	693
As (mg kg^{-1})	22.62	9.23	24.95	9.44	17.68	1.64
Ba (mg kg^{-1})	59.02	12.61	64.29	15.81	195.50	19.56
Ca (mg kg^{-1})	5570	1877	8284	4270	35837	10581
Co (mg kg^{-1})	9.46	2.80	10.82	2.52	8.51	1.03
Cr (mg kg^{-1})	42.62	17.36	37.49	9.20	74.19	14.51
Cu (mg kg^{-1})	21.62	4.20	20.75	4.52	222.47	49.74
Fe (mg kg^{-1})	34929	11191	42631	12194	40927	4052
Ga (mg kg^{-1})	4.77	2.55	3.13	1.97	5.08	0.74
Gd (mg kg^{-1})	2.60	1.15	2.94	1.42	1.12	1.10
K (mg kg^{-1})	1343	323	947	229	1271	197
La (mg kg^{-1})	15.33	3.85	15.75	4.22	14.95	1.73
Mg (mg kg^{-1}))	1708	403	1776	493	8917	1402
Mn (mg kg^{-1})	647	244	608	208	1765	242
Na (mg kg^{-1})	61.04	22.72	94.92	36.56	299.17	87.08
Nd (mg kg^{-1})	28.76	8.12	38.30	6.73	24.95	2.05
Ni (mg kg^{-1})	25.93	9.86	24.84	4.00	37.36	4.95
P (mg kg^{-1})	1354	374	1018	249	1319	160
Pb (mg kg^{-1})	30.98	7.83	26.47	7.18	107.45	17.62
Ti (mg kg^{-1})	23.98	10.63	21.61	8.39	79.26	20.57
V (mg kg^{-1})	52.19	18.60	53.18	15.06	59.75	3.84
Y (mg kg^{-1})	14.15	4.09	17.62	3.99	12.93	1.07
Yb (mg kg^{-1})	1.78	0.56	2.29	0.52	1.88	0.14
Zn (mg kg^{-1})	85.27	23.06	85.82	12.68	853.82	290.51
Zr (mg kg^{-1})	5.84	1.51	7.43	1.54	9.32	1.33

Table 3: Tracers failing the mass conservation test for each core and each correction.

	Sywell reservoir	Stanwick Lake	Kingsthorpe floodplain	Stanwick floodplain	Upton floodplain	Earls Barton floodplain
Uncorrected	χarm, ^{234}Th, ^{235}U, Ca, Gd, K, Ni, Ti	HIRM, ^{234}Th, ^{235}U, As, Ca, Co, Cr, Fe, Ga, La, Mn, Nd, P, Ti, V	HIRM, Cu, Ga, Gd, K, Nd, P	HIRM, ^{226}Ra, ^{228}Ac, ^{235}U, ^{212}Pb, Al, Cr, Cu, Fe, Gd, K, La, Mg, P, Ti	χarm, ^{226}Ra, ^{228}Ac, ^{235}U, ^{212}Pb, Al, As, Ga, Gd, K, La, Mg, P, V, Y, Yb, Zr	χlf, χfd, χarm, SIRM, IRM-100, HIRM, ^{228}Ac, ^{234}Th, ^{235}U, ^{212}Pb, Al, Co, Cu, Fe, Ga, Gd, La, Mn, Na, Nd, P, Ti, V, Y, Yb, Zr
Organic corrected	χarm, ^{235}U, Ca, Gd, Ni, Ti	IRM-100, HIRM, ^{226}Ra, ^{228}Ac, ^{234}Th, ^{235}U, ^{212}Pb, As, Ca, Co, Cr, La, Mn, Na, P, Ti	HIRM, ^{40}K, ^{234}Th, ^{235}U, Cu, Ga, Gd, K, Nd, P, Pb	IRM-100, ^{226}Ra, ^{228}Ac, ^{235}U, ^{212}Pb, Cr, Cu, Gd, K, La, Mg, Yb	χAarm, ^{226}Ra, ^{228}Ac, ^{235}U, ^{212}Pb, Al, As, Co, Gd, K, La, Mg, Nd, P, V, Y, Yb, Zr	χlf, χfd, χarm, SIRM, IRM-100, HIRM, ^{226}Ra, ^{228}Ac, ^{234}Th, ^{235}U, ^{212}Pb, Al, As, Co, Fe, Ga, Gd, K, La, Mn, Na, Nd, P, Ti, V, Y, Yb, Zr
Particle size corrected	χarm, HIRM, ^{40}K, Ba, Ca, Co, Cr, Ga, Gd, Mn, Nd, Ni, P, Ti, Y, Yb, Zn, Zr	χlf, IRM-100, HIRM, ^{40}K, ^{212}Pb, Al, As, Co, Cr, Fe, Ga, Gd, La, Mg, Mn, Nd, Ni, P, Ti, V, Y, Yb	HIRM, ^{234}Th, ^{235}U, Cu, Ga, Gd, Nd, P	SIRM, IRM-100, HIRM, ^{40}K, Al, Co, Cr, Cu, Fe, Gd, K, La, Mg, Na, Ni, P, Ti	χarm, ^{226}Ra, ^{228}Ac, ^{40}K, ^{235}U, Al, Ca, Fe, Gd, K, La, Mg, P	χlf, χfd, χarm, SIRM, IRM-100, HIRM, ^{40}K, ^{234}Th, ^{235}U, As, Co, Cr, Cu, Ga, K, La, Mn, Nd, P, Pb, Ti, V, Zn

Table 4: Tracers failing the Kruskal–Wallis H test (p=0.05) for each core and each correction.

	Uncorrected	Organic corrected	Particle size corrected
Upton Floodplain	-	-	As
Kingsthorpe Floodplain	Co, La, V	Co, Fe, La, V, Yb	Co, Fe, Y, Yb
Earls Barton Floodplain			Fe
Stanwick Floodplain	Ga, V	As, Co	
Sywell Reservoir	-	Co, Fe, La	-
Stanwick Lake	-	Fe	-

Table 5: The composite fingerprints, fingerprint discriminatory power and average goodness of fit of unmixing model outcomes.

Sywell reservoir

Uncorrected	Correctly classified (%)	Average Goodness of Fit	
Mag	81	0.74	χlf, χfd, SIRM, IRM-100, HIRM
Mag litho	81	0.95	χlf, χfd, ^{226}Ra, ^{40}K, ^{212}Pb
Mag geochem	94	0.92	χfd, Co, Fe, La, Mg, P, V, Yb, Zn
Geochem litho	91	0.94	^{226}Ra, Fe, La, Mg, P, V, Yb, Zr
Geochem	93	0.92	Cr, La, Mg, P, V, Yb, Zn
All	95	0.91	^{226}Ra, χfd, Fe, La, Mg, V, Yb, Zr
Organic corrected			
Geochem	91	0.55	Al, Gd, Mg, Nd, P, V, Yb

Stanwick lake

Uncorrected	Correctly classified (%)	Average Goodness of Fit	
Mag	<80		
Mag litho	81	0.75	χfd, χARM, SIRM, IRM-100, ^{212}Pb
Mag geochem	As 'All'		
Geochem litho	88	0.89	^{40}K, Al, Cu, K, Mg, Y
Geochem	88	0.94	Al, Ba, K, Yb, Zr
All	89	0.68	χfd, Al, K, Mg, Y, Zr

Kingsthorpe floodplain

Uncorrected	Correctly classified (%)	Average Goodness of Fit	
Mag	80	0.95	χlf, χfd, χarm, ,
Mag litho	81	0.63	χfd, Xarm, ^{228}Ac, ^{40}K,
Mag geochem	92	0.9	χarm, IRM-100, Ca, Mn, Y
Geochem litho	83	0.71	^{228}Ac, Ba, Ca, Cr, Ti
Geochem	86	0.91	Ba, Ca, Cr, Mg, Y, Zn
All	90	0.77	χlf, ^{212}Pb, Ca, Cr, Ti, Yb
Mag fallout*	87	0.93	^{137}Cs, Ca, Cr, Mg, Y
Geochem fallout*	83	0.88	^{137}Cs, χlf, χfd, χarm, SIRM
Organic corrected			
All	90	0.82	χlf, ^{212}Pb, Ca, Cr, Na, Ti, Y
Mag litho	82	0.71	χarm, IRM-100, ^{228}Ac, ^{212}Pb,
Geochem	83	0.91	Ba, Ca, Cr, Y, Zn

Earls Barton floodplain

Uncorrected	Correctly classified (%)	Average Goodness of Fit	
Mag	<80		
Mag litho	<80		
Mag geochem	<80		
Geochem litho	As "Geochem"		
Geochem	88	0.91	Ba, Ca, K, Mg, Pb, Zn
All	89	0.88	[40]K, Ba, Ca, K, Mg
Particle size corrected			
All	83	0.9	[228]Ac, [212]Pb, Al, Ba, Ca, Mg, Y

Upton floodplain

Uncorrected	Correctly classified (%)	Average Goodness of Fit	
Mag	<80		
Mag litho	82	0.75	χlf, χfd, SIRM, IRM-100, HIRM, [234]Th
Mag geochem	As 'All'		
Geochem litho	As "Geochem"		
Geochem	83	0.77	Co, Cu, Ni, Pb, Ti
All	90	0.55	χfd, Ba, Co, Cu, Pb
Organic corrected			
Mag litho	83	0.75	χlf, χfd, SIRM, IRM-100, HIRM, [234]Th
Geochem	81	0.77	Ba, Ca, Co, Cu, Pb, Ti
Particle size corrected			
Geochem	83	0.77	As, Co, Cu, Ti, Y

Stanwick floodplain

Uncorrected	Correctly classified (%)	Average Goodness of Fit	
Mag	<80		
Mag litho	<80		
Mag geochem	As 'All'		
Geochem litho	82	0.92	[234]Th, As, Ba, Co, Ni, V, Yb, Zr
Geochem	<80		
All	84	0.84	χfd, IRM-100, Ba, Ca, Co, Ni, Yb
Organic Corrected			
Geochem litho	82	0.76	Al, As, Ba, Ca, Co, Ni, Ti, Y
All	79	0.51	χlf, SIRM, IRM-100, Al, Ca, Na, Y
Particle size corrected			
Geochem litho	83	0.76	[226]Ra, [228]Ac, [234]Th, As, Ba, Mn, V, Yb, Zr
All	85	0.51	χlf, χarm, IRM-100, [226]Ra, Ca, Y, Zr

*Two additional Cs-137 containing tracer groups were included in the top 10 cm of the Kingsthorpe core, the use of this group is discussed in the following section.

Table 6: Mean percentage point differences between median tracer group predictions, with and without within source variability and discriminatory weightings.

	Mean difference between predictions (%)
Sywell Reservoir	
Mag litho (Weighted - Unweighted)	0.95
Geochem litho (Weighted - Unweighted)	1.22
Stanwick lake	
Mag litho (Weighted - Unweighted)	0.55
Geochem litho (Weighted - Unweighted)	5.64
Upton Floodplain	
Mag litho (Weighted - Unweighted)	0.14
Geochem litho (Weighted - Unweighted)	1.64
Stanwick floodplain	
Geochem litho (Weighted - Unweighted)	32.56
All (Weighted - Unweighted)	82.57
Geochem litho - All (Weighted - Weighted)	25.09
Geochem litho - All (Weighted - Unweighted)	62.21
All - Geochem litho (Weighted - Unweighted)	52.55
Kingsthorpe floodplain	
Mag (Weighted - Unweighted)	1.06
Mag litho (Weighted - Unweighted)	1.54
Mag Geochem (Weighted - Unweighted)	2.87
Geochem litho (Weighted - Unweighted)	7.75
Geochem (Weighted - Unweighted)	39.32
All (Weighted - Unweighted)	6.05
Geochem - Mag (Weighted - Weighted)	52.95
Geochem - Mag (Unweighted - Weighted)	13.63

Table 7: Pearson correlation coefficients (r) and associated p values for correlations between differences between tracer group predictions and LOI, SSA, and the χarm/Sirm and Sirm/χlf ratios. Statistically significant (p<0.05) values are highlighted in grey.

(A) Sywell Reservoir

		LOI	SSA	χarm/Sirm	Sirm/χlf
Mag - Mag litho	Correlation Coefficient	-.640	-.269	.009	-.592
	Sig. (2-tailed)	.000	.093	.956	.000
	N	40	40	40	40
Mag - Mag geochem	Correlation Coefficient	-.441	-.170	.189	-.491
	Sig. (2-tailed)	.004	.295	.244	.001

		LOI	SSA	χarm/Sirm	Sirm/χlf
	N	40	40	40	40
Mag - Geochem litho	Correlation Coefficient	-.087	-.117	-.109	.232
	Sig. (2-tailed)	.593	.474	.502	.149
	N	40	40	40	40
Mag - Geochem	Correlation Coefficient	.753	.184	-.118	.305
	Sig. (2-tailed)	.000	.255	.468	.056
	N	40	40	40	40
Mag - All	Correlation Coefficient	-.594	-.200	.341	-.421
	Sig. (2-tailed)	.000	.215	.031	.007
	N	40	40	40	40
Mag litho - Mag geochem	Correlation Coefficient	.209	-.175	.033	-.176
	Sig. (2-tailed)	.196	.279	.838	.277
	N	40	40	40	40
Mag litho - Litho geochem	Correlation Coefficient	-.090	-.389	.132	-.234
	Sig. (2-tailed)	.579	.013	.417	.147
	N	40	40	40	40
Mag litho - Geochem	Correlation Coefficient	-.402	-.153	-.075	-.598
	Sig. (2-tailed)	.010	.346	.644	.000
	N	40	40	40	40
Mag litho - All	Correlation Coefficient	.486	.098	-.219	.089
	Sig. (2-tailed)	.001	.546	.174	.587
	N	40	40	40	40
Mag geochem - Litho geochem	Correlation Coefficient	.167	-.272	.449	.210
	Sig. (2-tailed)	.304	.090	.004	.193
	N	40	40	40	40
Mag geochem - Geochem	Correlation Coefficient	-.692	-.219	.002	-.578
	Sig. (2-tailed)	.000	.174	.988	.000
	N	40	40	40	40
Mag geochem - All	Correlation Coefficient	-.546	-.261	.360	-.270
	Sig. (2-tailed)	.000	.104	.023	.092
	N	40	40	40	40
Litho geochem - Geochem	Correlation Coefficient	.472	-.024	.223	.367
	Sig. (2-tailed)	.002	.886	.166	.020
	N	40	40	40	40
Litho geochem - All	Correlation Coefficient	-.070	-.364	.515	.010
	Sig. (2-tailed)	.667	.021	.001	.950
	N	40	40	40	40
Geochem- All	Correlation Coefficient	-.753	-.178	.059	-.519
	Sig. (2-tailed)	.000	.272	.716	.001
	N	40	40	40	40

(B) Stanwick lake

		LOI	SSA	χarm/Sirm	Sirm/χlf
Mag litho - Geochem litho	Correlation Coefficient	.389	.358	.309	-.323
	Sig. (2-tailed)	.111	.145	.213	.191
	N	18	18	18	18
Mag litho - Geochem	Correlation Coefficient	.352	.376	.354	-.337
	Sig. (2-tailed)	.152	.124	.150	.171
	N	18	18	18	18
Mag litho - All	Correlation Coefficient	.030	-.332	-.024	.399
	Sig. (2-tailed)	.906	.179	.926	.101
	N	18	18	18	18
Geochem litho - Geochem	Correlation Coefficient	-.247	-.487	-.692	.298
	Sig. (2-tailed)	.324	.040	.001	.229
	N	18	18	18	18
Geochem litho - All	Correlation Coefficient	.352	.153	-.003	-.162
	Sig. (2-tailed)	.152	.543	.990	.521
	N	18	18	18	18
Geochem - All	Correlation Coefficient	.265	.371	.207	-.311
	Sig. (2-tailed)	.287	.130	.409	.210
	N	18	18	18	18

(C) Kingsthorpe floodplain

		LOI	SSA	χarm/Sirm	Sirm/χlf
Mag - Mag litho	Correlation Coefficient	.571	-.156	-.648	.797
	Sig. (2-tailed)	.002	.447	.000	.000
	N	26	26	26	26
Mag - Mag geochem	Correlation Coefficient	.545	-.087	-.796	.940
	Sig. (2-tailed)	.004	.673	.000	.000
	N	26	26	26	26
Mag - Geochem litho	Correlation Coefficient	-.062	-.082	.227	-.298
	Sig. (2-tailed)	.764	.690	.264	.139
	N	26	26	26	26
Mag - Geochem	Correlation Coefficient	-.354	-.097	.350	-.559

		LOI	SSA	χarm/Sirm	Sirm/χlf
	Sig. (2-tailed)	.076	.636	.080	.003
	N	26	26	26	26
Mag - All	Correlation Coefficient	-.582	.264	.468	-.657
	Sig. (2-tailed)	.002	.192	.016	.000
	N	26	26	26	26
Mag litho - Mag geochem	Correlation Coefficient	.289	-.028	-.620	.783
	Sig. (2-tailed)	.152	.892	.001	.000
	N	26	26	26	26
Mag litho - Geochem litho	Correlation Coefficient	-.247	-.022	.460	-.567
	Sig. (2-tailed)	.223	.917	.018	.003
	N	26	26	26	26
Mag litho - Geochem	Correlation Coefficient	-.447	.027	.515	-.723
	Sig. (2-tailed)	.022	.897	.007	.000
	N	26	26	26	26
Mag litho - All	Correlation Coefficient	-.564	.250	.529	-.718
	Sig. (2-tailed)	.003	.218	.005	.000
	N	26	26	26	26
Mag geochem - Geochem litho	Correlation Coefficient	-.446	.083	.715	-.887
	Sig. (2-tailed)	.022	.685	.000	.000
	N	26	26	26	26
Mag geochem - Geochem	Correlation Coefficient	-.574	.074	.718	-.895
	Sig. (2-tailed)	.002	.721	.000	.000
	N	26	26	26	26
Mag geochem - All	Correlation Coefficient	-.531	.191	.648	-.851
	Sig. (2-tailed)	.005	.349	.000	.000
	N	26	26	26	26
Geochem litho - Geochem	Correlation Coefficient	-.591	.066	.252	-.432
	Sig. (2-tailed)	.001	.750	.214	.027
	N	26	26	26	26
Geochem litho - All	Correlation Coefficient	-.637	.321	.405	-.559
	Sig. (2-tailed)	.000	.110	.040	.003
	N	26	26	26	26
Geochem - All	Correlation Coefficient	-.652	.354	.468	-.602
	Sig. (2-tailed)	.000	.076	.016	.001
	N	26	26	26	26

(D) Upton floodplain

		LOI	SSA	χarm/Sirm	Sirm/χlf
Mag - Mag litho	Correlation Coefficient	.019	-.019	-.101	-.002
	Sig. (2-tailed)	.949	.949	.730	.994
	N	14	14	14	14
Mag - Geochem	Correlation Coefficient	.871	-.571	-.240	-.081
	Sig. (2-tailed)	.000	.033	.409	.782
	N	14	14	14	14
Mag - All	Correlation Coefficient	.415	-.355	-.198	.141
	Sig. (2-tailed)	.140	.212	.497	.631
	N	14	14	14	14
Mag litho - Geochem	Correlation Coefficient	.871	-.571	-.240	-.081
	Sig. (2-tailed)	.000	.033	.409	.782
	N	14	14	14	14
Mag litho - All	Correlation Coefficient	.362	-.358	-.277	.198
	Sig. (2-tailed)	.203	.209	.337	.497
	N	14	14	14	14
Geochem - All	Correlation Coefficient	-.878	.573	.253	.068
	Sig. (2-tailed)	.000	.032	.383	.817
	N	14	14	14	14

(E) Earls Barton floodplain (an χarm measurement was unavailable for this core due to equipment failure)
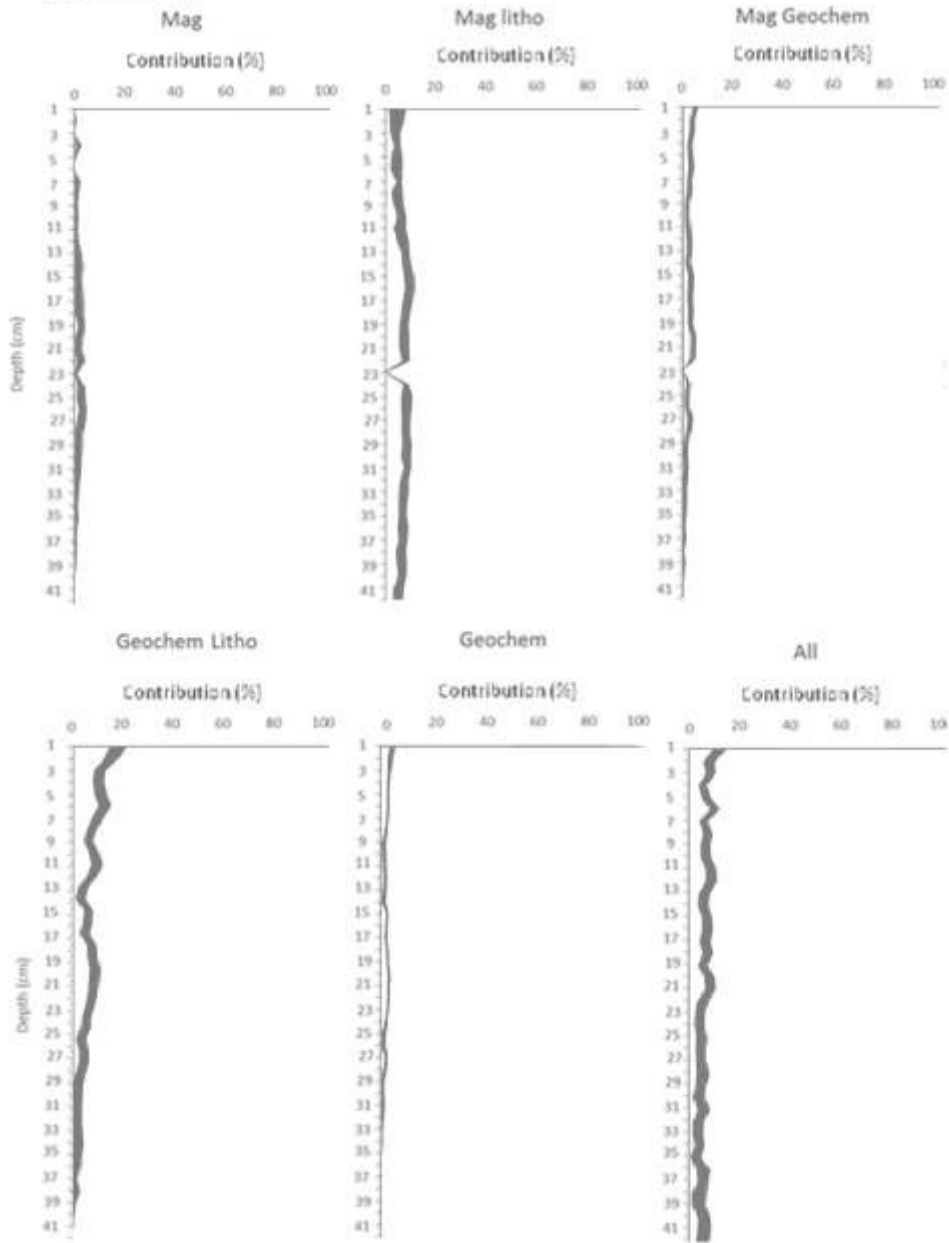
		LOI	SSA
All - Geochem	Correlation Coefficient	.239	-.809
	Sig. (2-tailed)	.173	.000
	N	34	34

(F) Stanwick floodplain

		LOI	SSA	χarm/Sirm	Sirm/χlf
Geochem litho - All	Correlation Coefficient	-.790	.876	.783	-.812
	Sig. (2-tailed)	.000	.000	.000	.000
	N	31	31	31	31

ONLINE SUPPLIMENTARY MATERIAL

(A) Sywell Reservor
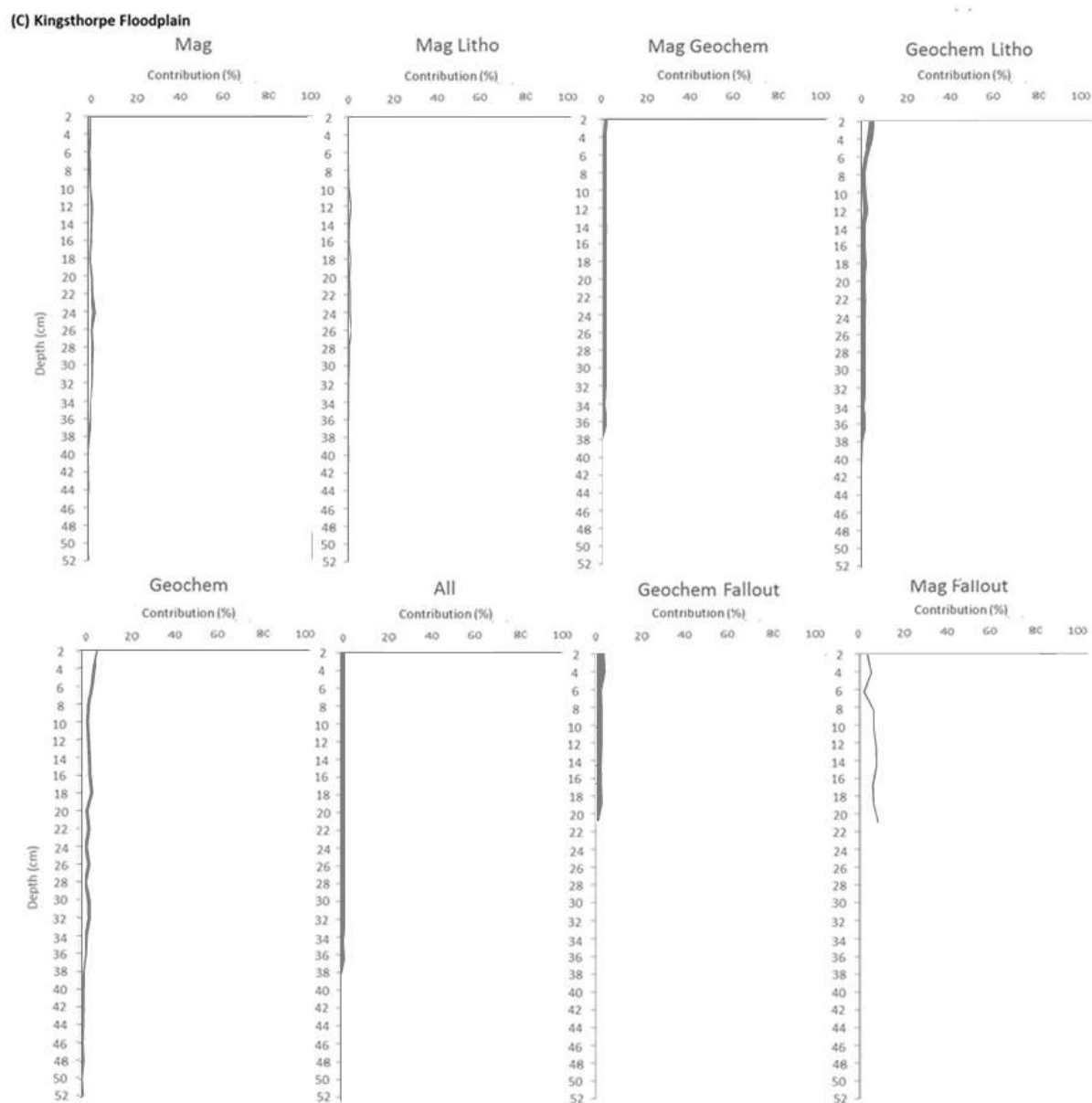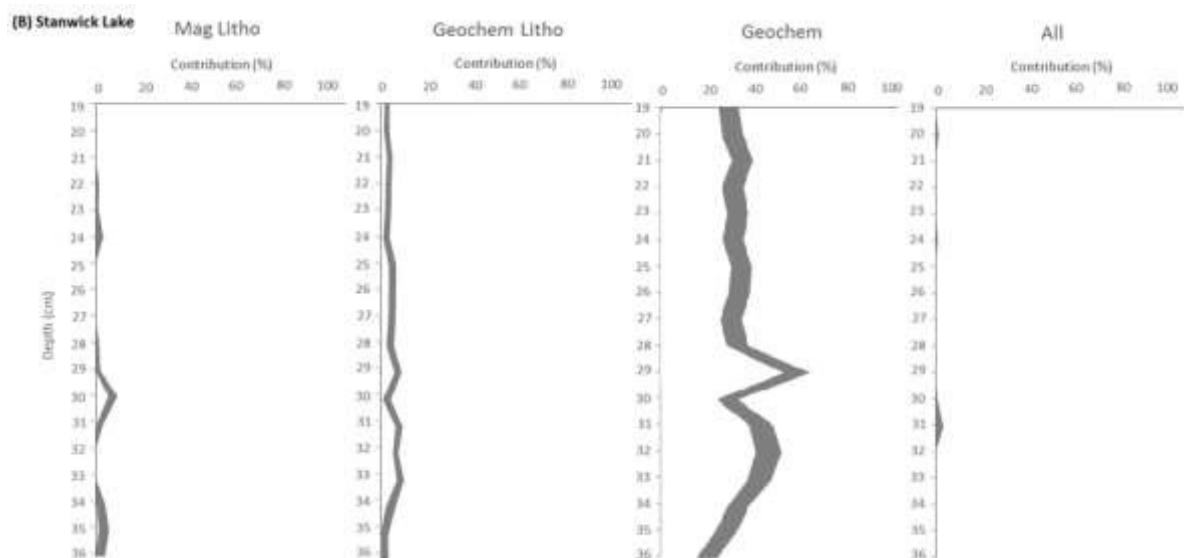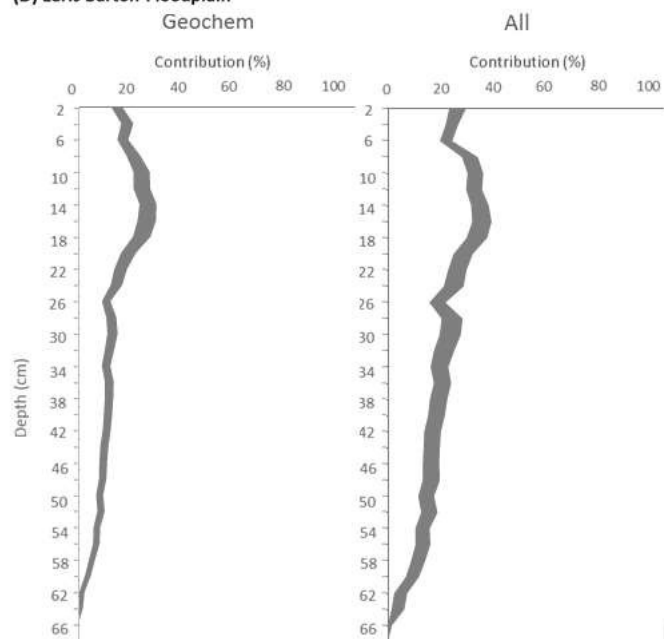
(B) Stanwick Lake

Mag Litho · Geochem Litho · Geochem · All

(C) Kingsthorpe Floodplain

Mag · Mag Litho · Mag Geochem · Geochem Litho

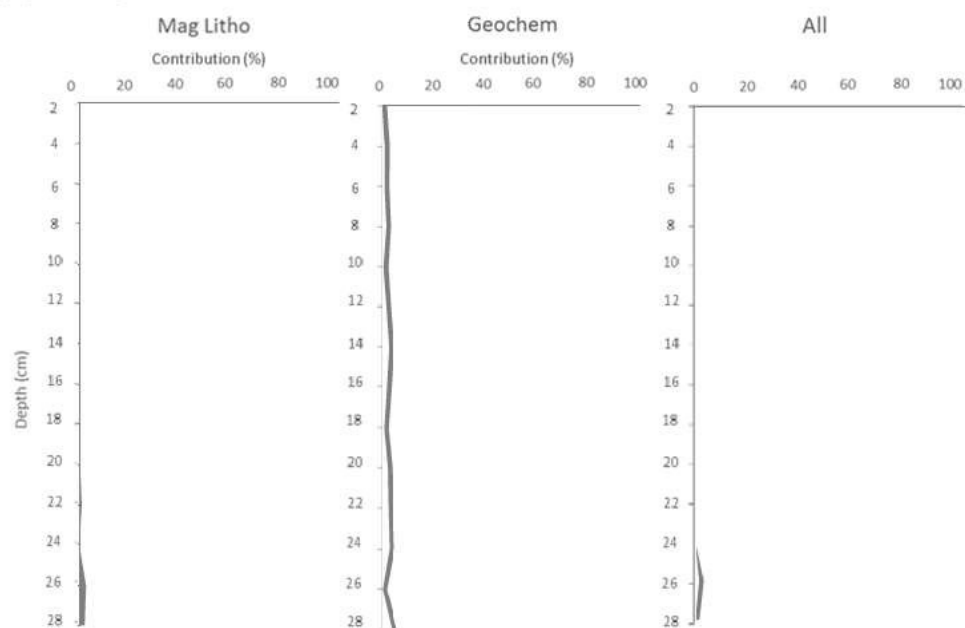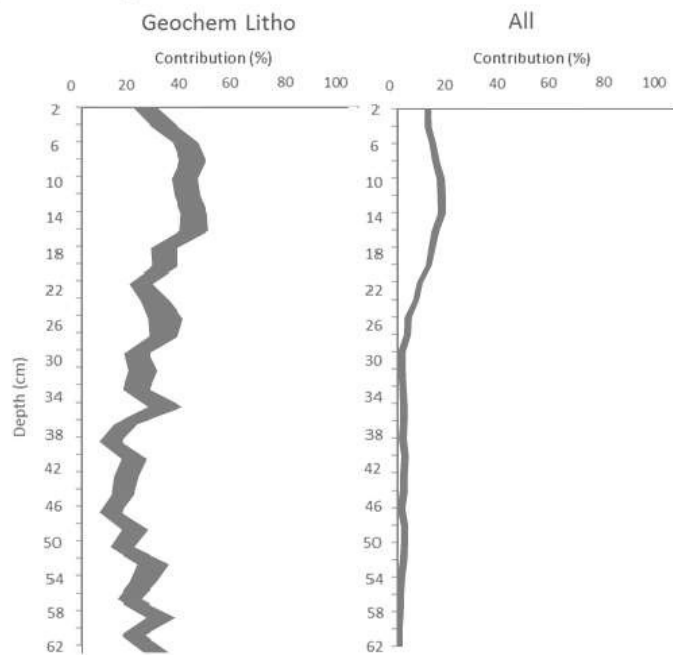Geochem · All · Geochem Fallout · Mag Fallout

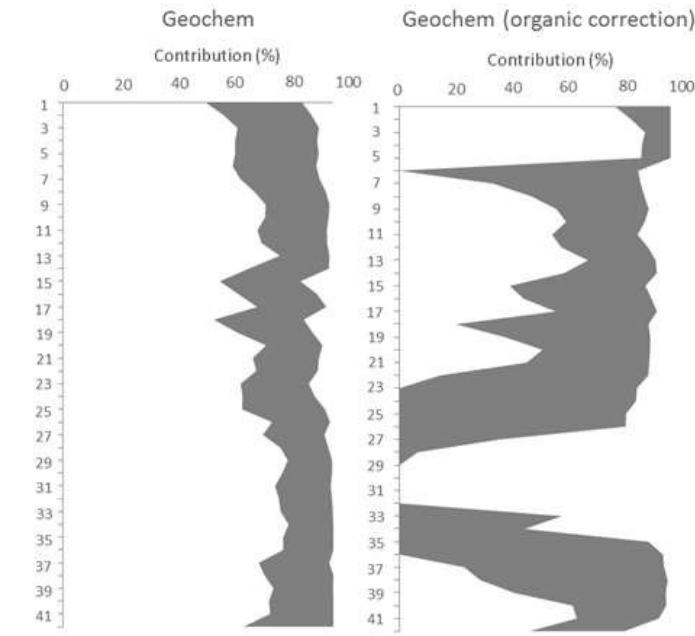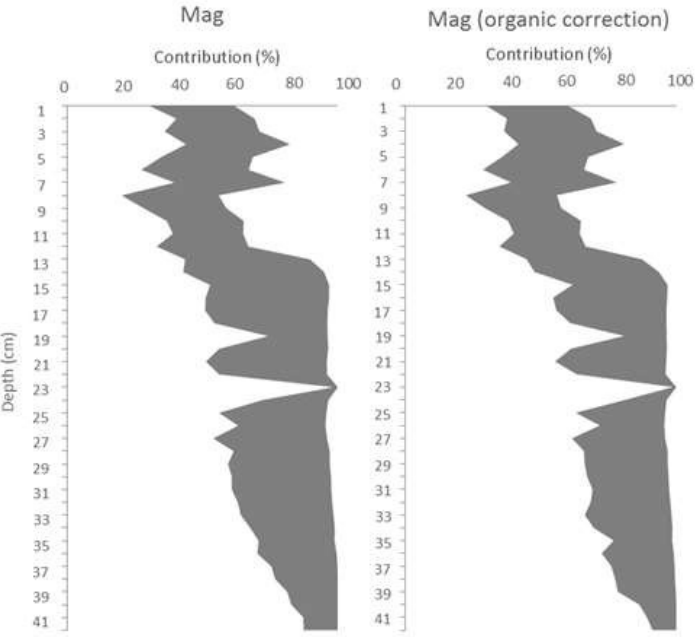**(D) Earls Barton Floodplain**

(E) Upton Floodplain

(F) Stanwick Floodplain

Supplementary figure 1: Predicted contributions of sediment originating from urban street dusts made by the different tracer groups, the grey area represents the range between the 25th and 75th percentile predicted contributions.

(A) Sywell Reservoir

Mag

Contribution (%)

Mag (organic correction)

Contribution (%)

Geochem

Contribution (%)

Geochem (organic correction)

Contribution (%)

Depth (cm)

(B) Stanwick Lake — Mag Litho; Mag Litho (organic correction). Contribution (%) versus Depth (cm).
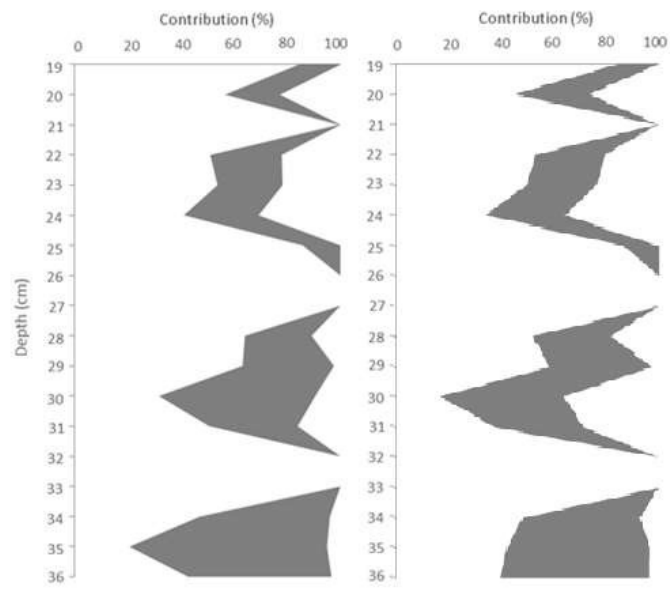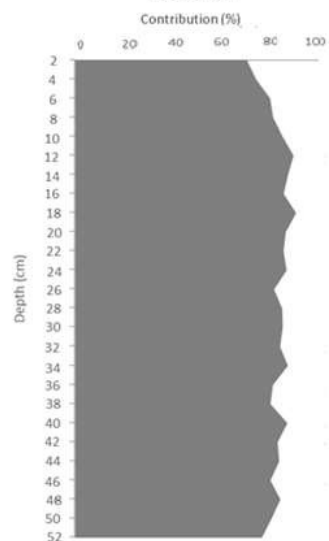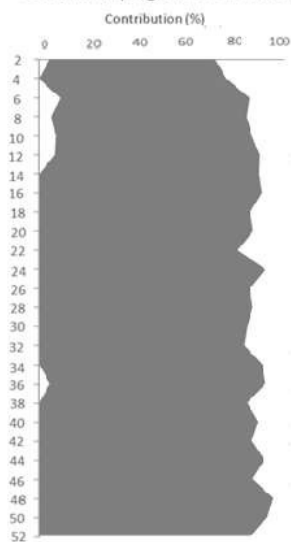
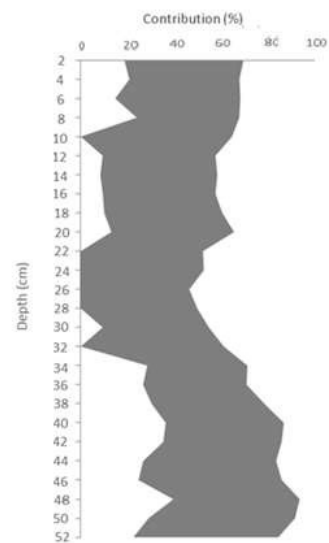**(C) Kingsthorpe Floodplain**
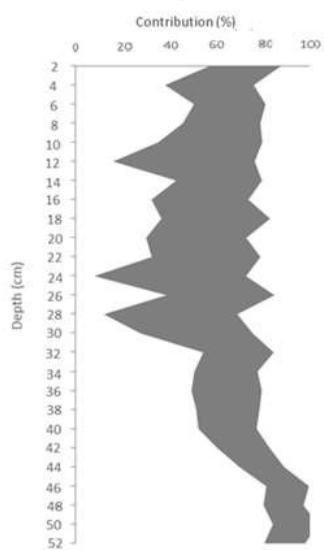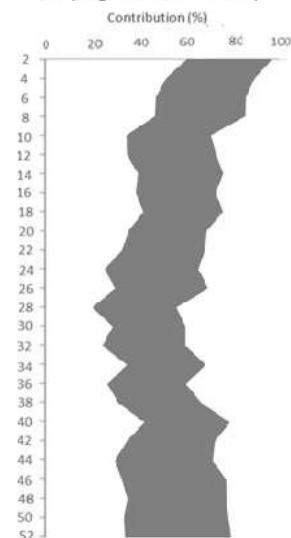
Mag Litho

Mag Litho (organic correction)
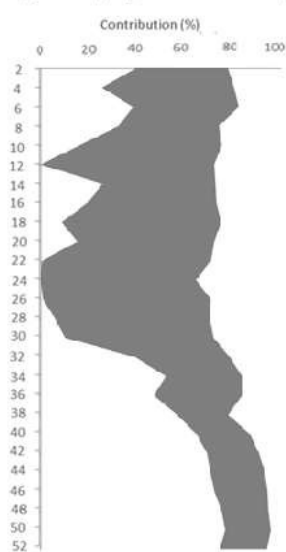
Geochem

Geochem (organic correction)

All

All (organic correction)

(D) Earls Barton Floodplain

(E) Upton Floodplain

Mag Litho

Mag Litho (organic correction)

Geochem

Geochem (organic correction)
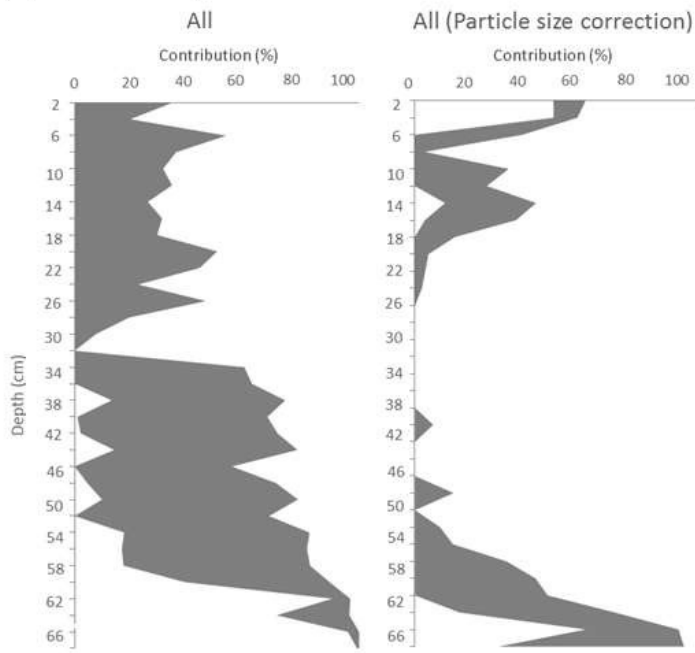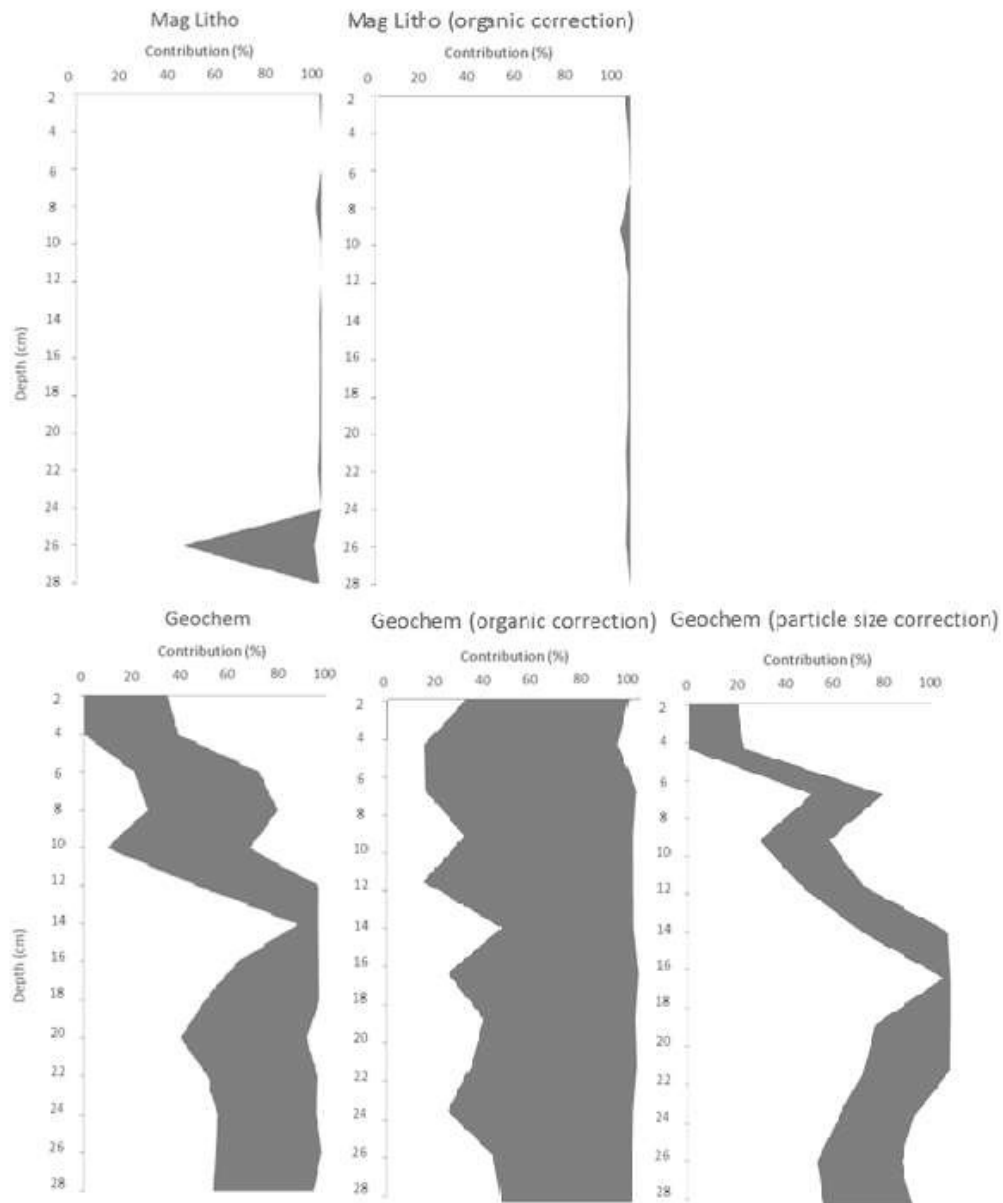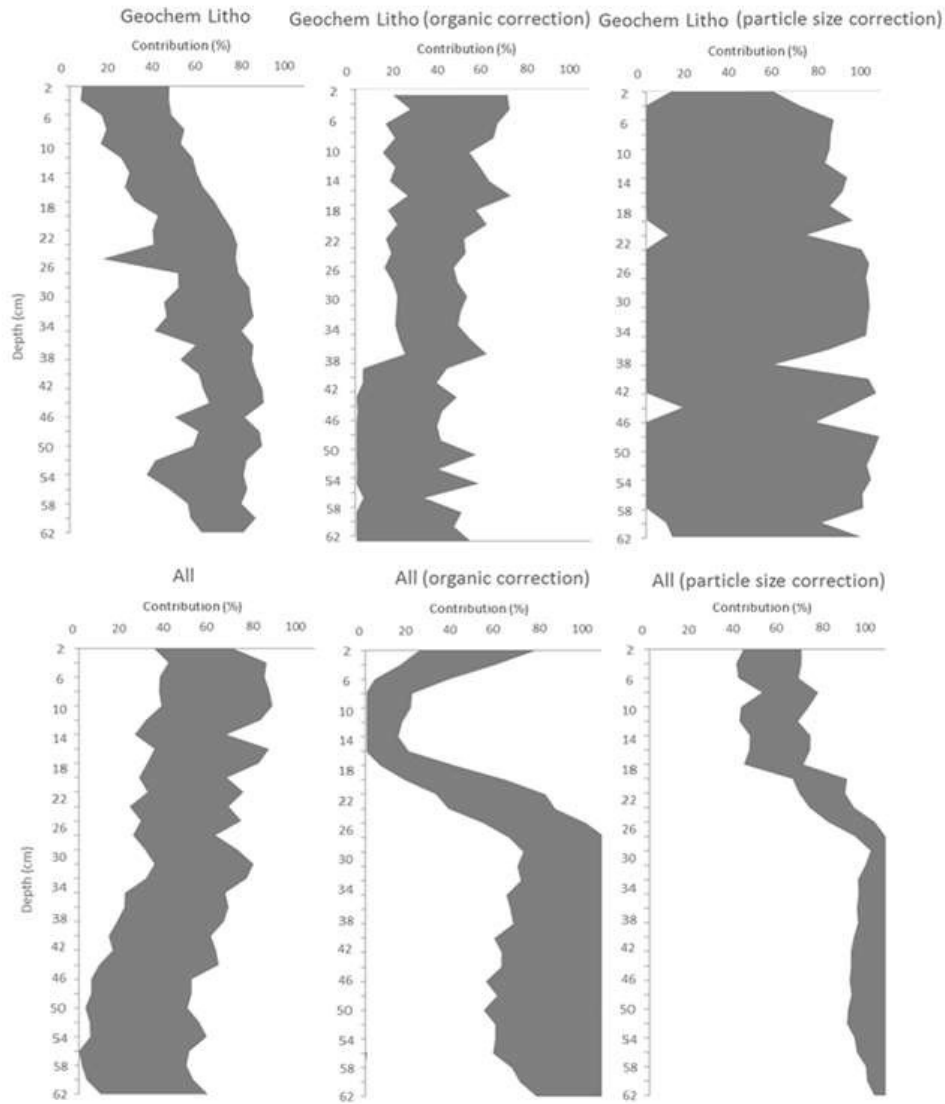
Geochem (particle size correction)

Supplementary figure 2: The impacts of organic matter and particle size corrections on modelling results, the grey area represents the range between the 25th and 75th percentile predicted contributions.

(A) Sywell Reservoir
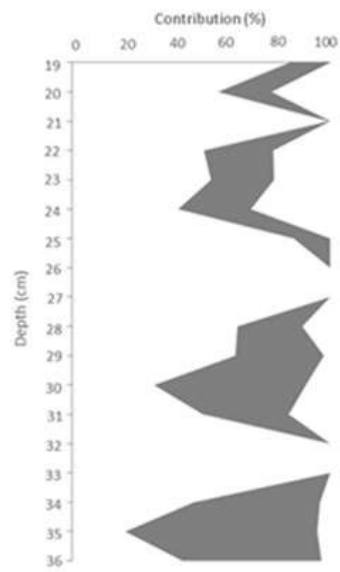
Mag litho

Mag litho (no weightings)

Geochem Litho
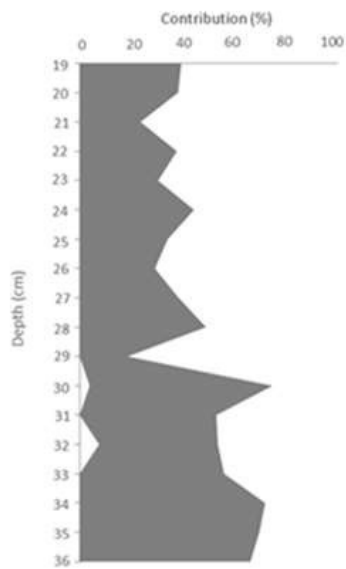
Geochem Litho (no weightings)

(B) Stanwick Lake

Mag Litho

Contribution (%)

Mag Litho (no weightings)

Contribution (%)

Geochem Litho

Contribution (%)

Geochem Litho (no weightings)

Contribution (%)

Mag

Mag (no weightings)

Mag Litho

Mag Litho (no weightings)

Mag Geochem

Mag Geochem (no weighting)

Geochem Litho

Geochem Litho (no weightin)

Geochem

Geochem (no weightings)

All

All (no weightings)

(E) Upton Floodplain

Mag Litho

Mag Litho (no weightings)

Geochem

Geochem (no weightings)
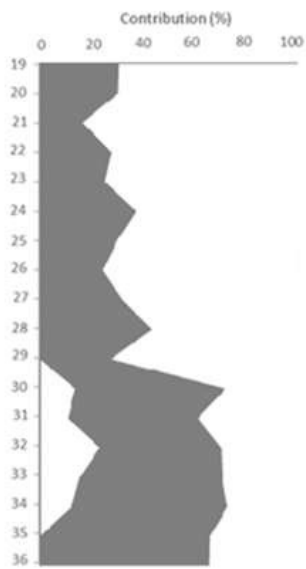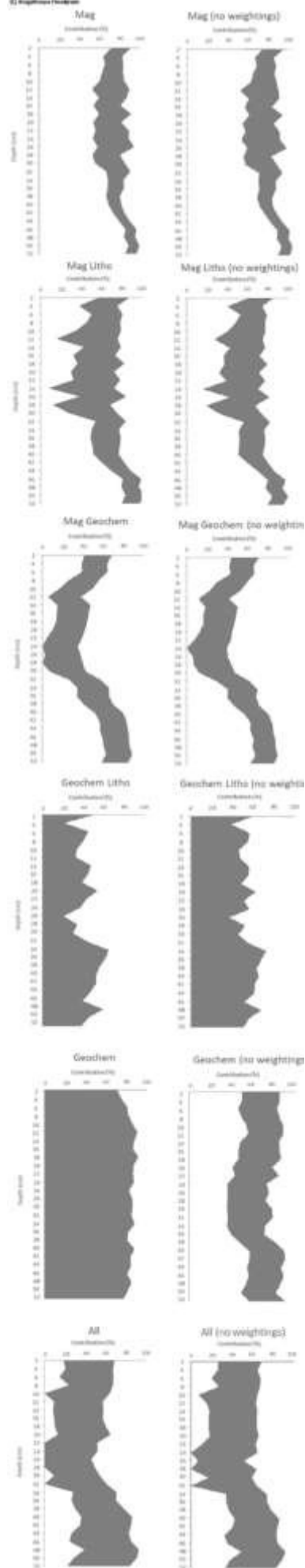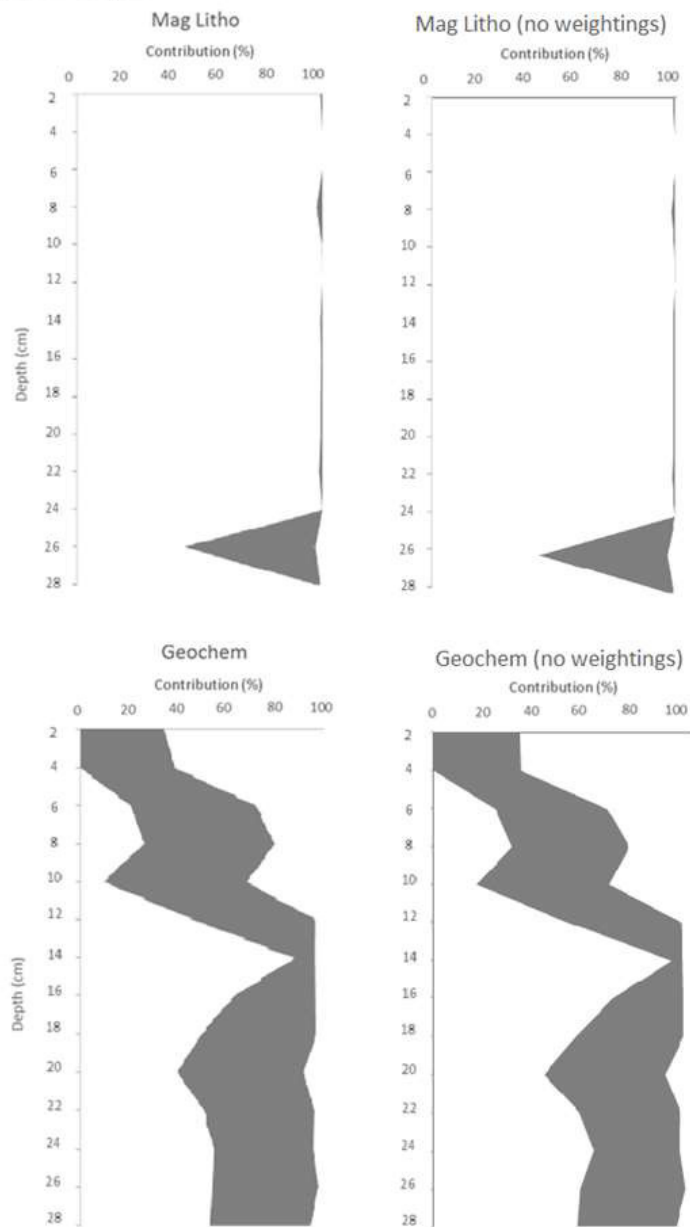
(F) Stanwick Floodplain
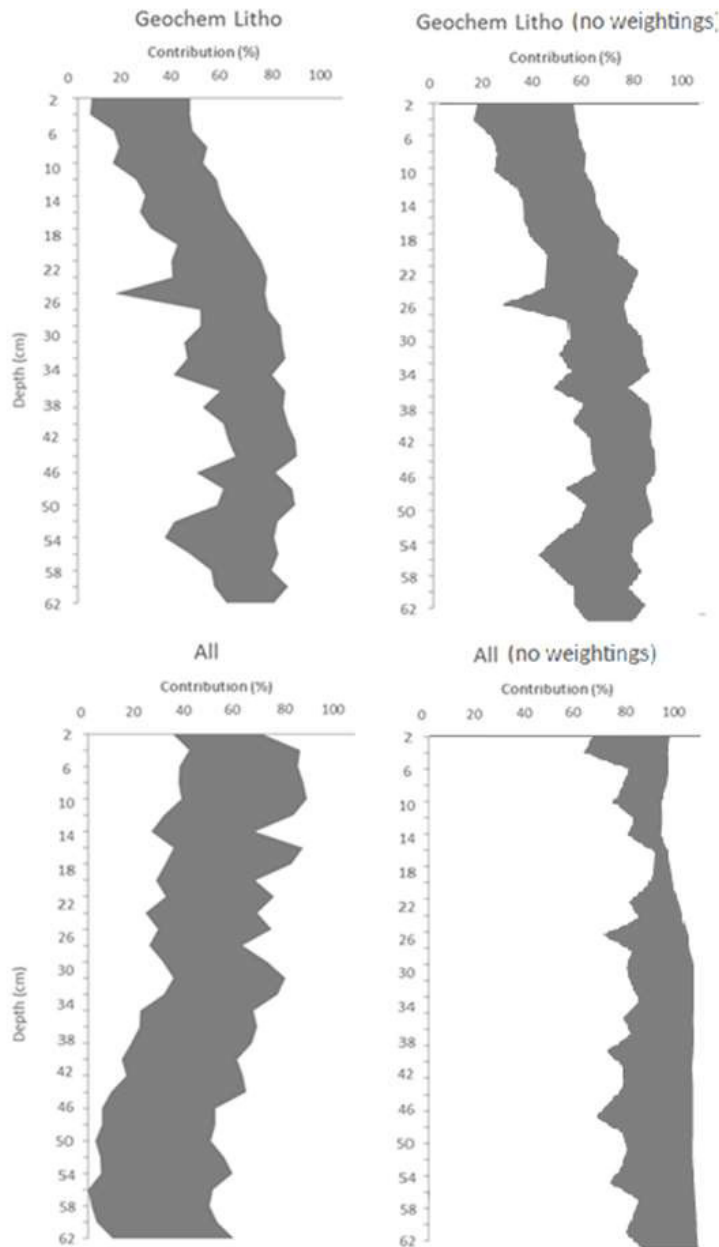
Supplementary figure 3: The impacts of weightings for tracer discriminatory and within source variability on modelling results, the grey area represents the range between the 25th and 75th percentile predicted contributions.
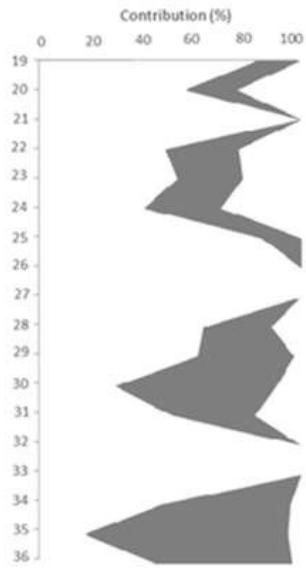
Supplementary table 1: Distribution of sediment source sampling across the different land uses and geologies of the Nene basin.

	White Sands	Unclassified	Silts and Clays	Sandstone Siltstone and Mudstone	Sand and Ironstone	Sand and Gravel	Mudstone	Marlstone	limestone	Ferrugnious Lime and Ironstone	Disturbed land	Diamicton	Clay Silt Sand Gravel	Total

Source														
Surface agricultural sources (total)	247	21	43	5	2	12	15	53	22	39	1	26	3	5
Surface agricultural sources (Cultivated land)	173	14	34	5	1	10	14	37	12	25	1	18	2	0
Surface agricultural sources (Grassland)	74	7	9	0	1	2	1	16	10	14	0	8	1	5
Channel Banks	65													
Urban street dusts	21													

Supplementary table 2: W_i and SV_{si} correction factors for the Stanwick floodplain core, factors did not vary significantly in the other cores fingerprinted.

Tracer	Uncorrected		Organic correted		Particle size corrected	
	W_i	SV_{si}	W_i	SV_{si}	W_i	SV_{si}
χlf	2.91	0.74	3.61	0.75	3.06	0.70
χfd	2.57	0.56	3.23	0.56	2.74	0.54
χarm	2.37	0.61	2.80	0.61	2.60	0.58
IRM1T	2.80	0.68	3.31	0.68	2.93	0.68
IRM-100	2.82	0.64	3.32	0.65	3.17	0.51
HIRM	2.69	0.77	3.34	0.77	2.72	0.77
[226]Ra	2.47	0.72	2.72	0.74	1.92	0.71
[137]Cs	2.91	0.33	3.54	0.44	2.76	0.57
[228]Ac	2.84	0.78	3.12	0.81	2.19	0.77
[40]K	2.44	0.86	2.69	0.87	1.46	0.84
[234]Th	3.00	0.75	3.76	0.75	2.67	0.76
[235]U	1.79	0.61	2.05	0.61	1.62	0.62
[212]Pb	2.55	0.86	2.72	0.84	1.65	0.84
Al	1.75	0.85	2.76	0.84	2.47	0.85
As	2.02	0.72	2.43	0.72	1.73	0.73
Ba	3.62	0.81	4.34	0.79	3.56	0.78
Ca	4.01	0.62	4.85	0.60	3.95	0.62
Co	3.47	0.78	1.05	0.79	2.76	0.76
Cr	2.04	0.72	2.78	0.73	2.35	0.70
Cu	2.67	0.79	3.36	0.78	2.61	0.78
Fe	1.80	0.77	2.67	0.76	1.25	0.75
Ga	2.77	0.57	1.38	0.56	1.47	0.56
Gd	2.11	0.38	2.48	0.36	2.04	0.46
K	2.93	0.79	3.52	0.79	2.28	0.79

La	2.05	0.79	2.67	0.80	1.42	0.79
Mg	3.41	0.78	4.06	0.80	3.40	0.76
Mn	2.07	0.71	2.80	0.71	2.51	0.71
Na	3.78	0.65	4.68	0.64	3.86	0.63
Nd	1.27	0.82	1.41	0.81	1.00	0.80
Ni	1.38	0.78	1.96	0.77	1.80	0.77
P	2.69	0.78	3.18	0.77	1.96	0.79
Pb	2.53	0.77	3.12	0.78	2.45	0.72
Ti	2.62	0.64	3.41	0.64	2.69	0.59
V	2.26	0.77	1.52	0.76	1.19	0.78
Y	1.31	0.81	1.27	0.81	3.38	0.80
Yb	1.00	0.79	1.00	0.79	2.92	0.79
Zn	2.66	0.75	3.23	0.72	2.61	0.67
Zr	3.57	0.81	4.36	0.80	3.49	0.79

Supplementary table 3: Mean percentage point differences between the median predictions of the different tracer groups.

Sywell Reservoir	Mag litho	Mag Geochem	Geochem litho	Geochem	All
Mag	24.65	19.00	16.10	16.34	23.64
Mag litho		14.92	20.24	33.49	10.40
Mag Geochem			14.75	21.82	8.09
Geochem litho				22.50	18.83
Geochem					27.55

Kingsthorpe Floodplain	Mag litho	Mag Geochem	Geochem litho	Geochem	All
Mag	14.85	31.30	53.66	39.57	33.96
Mag litho		17.11	39.81	28.47	22.58
Mag Geochem			27.91	24.65	24.79
Geochem litho				15.30	21.51
Geochem					15.06

Earls Barton Floodplain	Geochem
All	17.33

Upton Floodplain	Mag litho	Geochem	All
Mag	1.09	37.67	1.94
Mag litho		36.81	1.64

Geochem 37.89

**Stanwick
Floodplain** **All**
Geochem litho 34.03

Supplementary table 4: Mean percentage point differences between the median predictions of the different tracer groups with and without organic matter and particle size corrections.

Sywell Reservoir	Mag	Geochem	Geochem (Organic corrected)
Mag		16.34	29.99
Mag (Organic corrected)	1.19	14.75	30.48
Geochem	16.34		23.82

Stanwick lake	Mag litho	Geochem	All
Mag litho		64.58	5.60
Mag litho (Organic corrected)	5.79	59.24	4.67

Earls Barton Floodplain	All	Geochem litho
All		17.33
All (Particle size corrected)	18.87	23.41

Upton floodplain	Mag litho	Geochem	Geochem (Organic corrected)	Geochem (Particle size corrected)
Mag litho		36.81	24.52	40.49
Mag litho (Organic corrected)	0.14	37.48	24.38	40.35

Stanwick floodplain	Geochem litho	All	All (Organic corrected)	All (Particle size corrected)
Geochem litho		25.09	14.57	27.96
Geochem litho (Organic corrected)	28.30	39.35	41.12	29.03
Geochem litho (Particle size corrected)	11.03	19.61	17.60	32.74
All	25.09		30.34	42.51
All (Organic corrected)	14.57	30.34		41.75
All (Particle size corrected)	27.96	42.51	41.75	

Kingsthorpe Floodplain	Mag litho	Geochem	All	Mag litho (Organic corrected)	Geochem (Organic corrected)	All (Organic corrected)
Mag litho		33.49	10.40	6.61	25.20	14.93
Geochem	33.49		27.55	39.46	17.08	28.11
All	10.40	27.55		22.11	14.05	15.11
Mag litho (Organic corrected)	**6.61**	39.46	22.11		22.98	14.19
Geochem (Organic corrected)	**25.20**	17.08	14.05	22.98		12.15